Maternal *almondex*, a neurogenic gene, is required for the proper subcellular distribution of Notch in early embryogenesis of *Drosophila*

A dissertation submitted to

DEPARTMENT OF BIOLOGICAL SCIENCES,

GRADUATE SCHOOL OF SCIENCE,

OSAKA UNIVERSITY

In fulfillment of the requirements for the degree of

DOCTOR OF PHILOSOPHY

By

Puspa DAS

December, 2019

Thesis Title in Japanese

母性 **neurogenic** 遺伝子 ***almondex*** はショウジョウバ

エ初期胚における**Notch**の正常な細胞内分布に必要である

(ぼせい neurogenic いでんし *almondex*
はショウジョウバエしょきはいにおける Notch のせいじょうなさい
ぼうないぶんぷにひつようである)

Chief Examiner: Professor Kenji MATSUNO (Department of Biological Sciences,
Graduate School of Science, Osaka University)
Second Readers: Professor Masahiro UEDA (Department of Biological Sciences,
Graduate School of Science, Osaka University)
Professor Joji MIMA (Institute of Protein Research, Osaka University)
Professor Motoo KITAGAWA (Department of Biochemistry,
International University of Health and Welfare,
School of Medicine, Narita, Chiba, Japan

Preface

This study was conducted under the supervision of Professor Kenji Matsuno at the Department of Biological Sciences, Graduate School of Science, Osaka University, from 2016-2019.

In this study, I aimed to study the roles of Almondex, an evolutionarily conserved double-pass transmembrane protein, encoded by *Drosophila almondex*, in early neurogenesis of *Drosophila* embryos. *Drosophila almondex* has been identified as a maternal effect gene that regulates Notch signaling in the 1970s in certain contexts but its mechanistic function has been obscure. I found that *almondex* is partially required for Notch signaling dependent *single-minded* expression in the mesoectoderm as well as for the proper subcellular distribution of the Notch receptor at a specific time window of development, at the mid-stage 5, in the neuroectoderm. Taken together, I speculate that *almondex* may facilitate Notch activation by regulating the intracellular distribution of Notch receptor during early embryogenesis of *Drosophila*.

Almondex are evolutionary conserved from *Drosophila* to human. Therefore, the findings from my study will provide general as well as new concepts regarding roles of Almondex in Notch signaling across species.

Puspa DAS

Laboratory of Cell Biology (Matsuno Lab.)

Department of Biological Sciences, Graduate School of Science, Osaka University

1-1 Machikaneyama, Toyonaka, Osaka, 560-0043 JAPAN

Index

Abstract

Notch signaling plays crucial roles in the control of cell fate and physiology through local cell–cell interactions. The core processes of Notch signal transduction are well established, but the mechanisms that fine-tune the pathway in various developmental and post-developmental contexts are less clear. *Drosophila almondex*, which encodes an evolutionarily conserved double-pass transmembrane protein, was identified in the 1970s as a maternal-effect gene that regulates Notch signaling in certain contexts, but its mechanistic function remains obscure. In this study, we examined the role of *almondex* in Notch signaling during early *Drosophila* embryogenesis. We found that in addition to being required for lateral inhibition in the neuroectoderm, *almondex* is also partially required for Notch-signaling-dependent *single-minded* expression in the mesectoderm. Furthermore, we found that *almondex* is required for proper subcellular Notch receptor distribution in the neuroectoderm, specifically during mid-stage 5 development. The absence of maternal *almondex* during this critical window of time caused Notch to accumulate abnormally in cells in a mesh-like pattern. This phenotype did not include any obvious change in subcellular Delta ligand distribution, suggesting that it does not result from a general vesicular-trafficking defect. Considering that dynamic Notch trafficking regulates signal output to fit the specific context, we speculate that *almondex* may facilitate Notch activation by regulating intracellular Notch receptor distribution during early embryogenesis.

Key words: *almondex*, Notch, Neurogenesis, Notch signaling, Trafficking, *Drosophila*

1. Introduction

Cell-cell communication plays many crucial roles in development and tissue homeostasis in metazoans, which are mediated through many cell signaling pathways that are evolutionarily conserved. In such cell signaling pathways, either cells can interact through direct and local cell-cell contact, such as Notch signaling or are mediated by secretory and diffusible ligand molecules that interacts through intracellular space, such as Wnt, Hedgehog and TGFβ/BMP signaling. Notch signaling is a highly conserved cell signaling pathway in metazoans, where a family of receptor proteins, Notch receptors transduces signal to its ligands through direct cell-cell contacts (Artavanis-Tsakonas, 1995; Kopan & Ilagan, 2009; Yamamoto et al., 2014) (Figure 1).

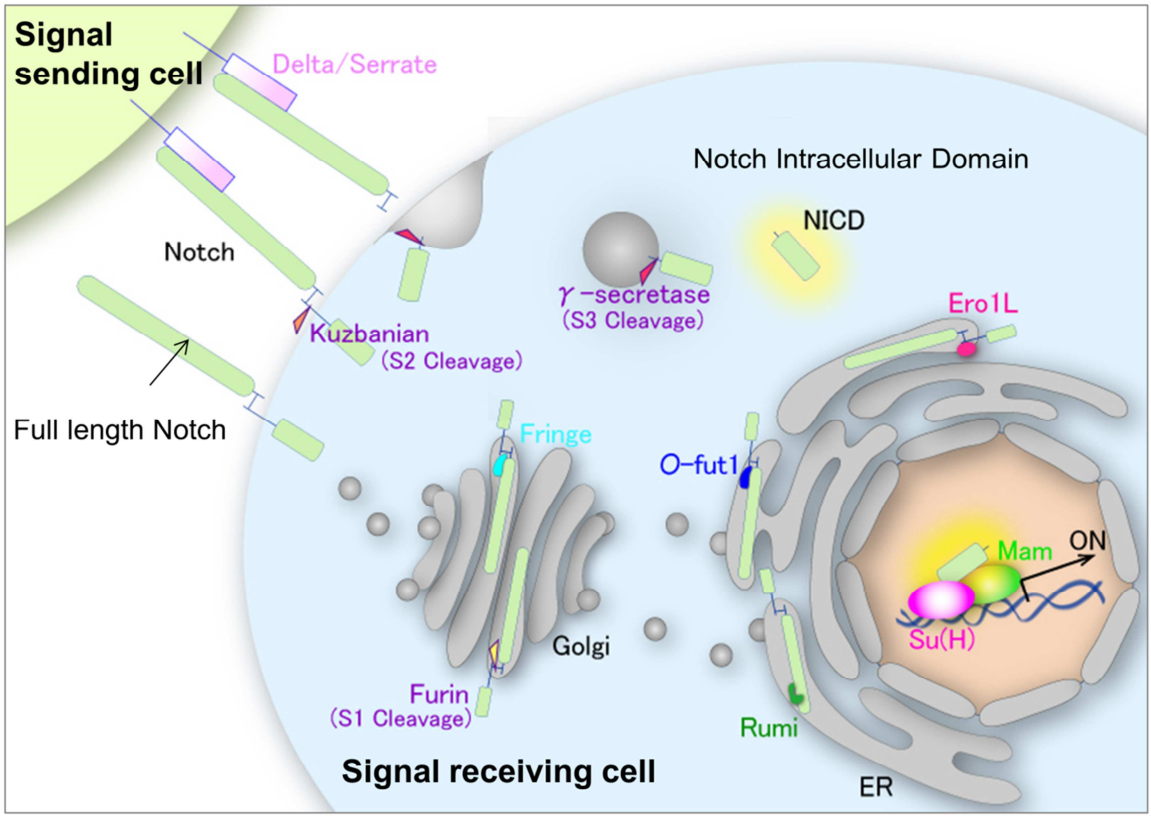

Figure 1: Overview of the Notch signaling pathway

The core components of the Notch signaling and their functions are evolutionarily conserved in metazoans (Artavanis-Tsakonas, 1995; Guruharsha et al., 2012). The Notch pathway controls a large variety of cell-type specifications and cell physiology (Artavanis-Tsakonas, 1995, 1999; Bray, 2006; Kopan & Ilagan, 2009). As Notch signaling is a core pathway that involved in many cell fate decisions, it is not surprising that defective Notch signaling results a number of developmental diseases as well as cancer in human including T-ALL (T-cell acute lymphoblastic leukemia), CADASIL (Cerebral Autosomal-Dominant Arteriopathy with Sub-cortical Infarcts and Leukoencephalopathy), Multiple Sclerosis (MS), Tetralogy of Fallot, Alagille syndrome (Sharma, 2007; Louvi & Artavanis-Tsakonas, 2012; Siebel & Lendahl, 2017; Salazar & Yamamoto, 2018). In addition, inhibition of Notch signaling has been shown to have anti-proliferative effects on T-cell acute lymphoblastic leukemia in cultured cells and in a mouse model (Moellering et al., 2009; Arora & Ansari, 2009). It has also been found that Rex1 has inhibitory effects on the expression of Notch in mesenchymal stem cells, preventing differentiation (Bhandari et al., 2010).

Both Notch receptors (N) and their ligands contain a distinct type 1, single-pass transmembrane domain, which essentially conserved across many species in vertebrates (Vassin et al., 1987; Johansen et al., 1989; Kidd et al., 1989; Rebay et al., 1991; Artavanis-Tsakonas, 1995; Kopan & Ilagan, 2009) (Figure 2). *Drosophila* contain a single Notch protein, *C. elegans* contain two redundant Notch paralogs, Lin-12 and GLP-1, and humans have four Notch variants, Notch 1-4 (Greenwald, 1983; Austin, 1987; Austin, 1989). The protein can broadly be split into the Notch extracellular domain (NECD) and Notch intracellular domain (NICD) that joined together by a

single-pass transmembrane domain (TM). The NECD contains 36 epidermal growth factor (EGF)-like repeats in *Drosophila*, 28-36 in humans, and 13 and 10 in *C. elegans* Lin-12 and GLP-1 respectively, some of which are used to physically bind to its ligands (Greenwald, 1985; Wharton, 1985; Rebay et al., 1991, Gordon et al., 2008; Kovall et al., 2017; Yamamoto, 2019). To the EGF-like repeats of Notch, various *O*-glycans, which modulate the binding affinity to distinct types of ligands and are required for proper intracellular trafficking of Notch (Logeat et al., 1998; Rana and Haltiwanger, 2011). EGF repeats 11-12 on the NECD have been shown to be necessary and sufficient for trans-signaling interactions between Notch and its ligands (Rebay et al., 1991). Additionally, EGF repeats 24-29 have been implicated in inhibition of cis-interactions between Notch and ligands co-expressed in the same cell (de Celis, 2000). The EGF repeats are followed by three cysteine-rich Lin-12/Notch Repeats (LNR) and a heterodimerization (HD) domain. Together the LNR and HD compose the negative regulatory region (NRR) adjacent to the cell membrane and help prevent signaling in the absence of ligand binding. During the maturation of Notch, NECD is cleaved by Furin within the NRR in the extracellular domain (S1 site), and two cleaved fragments are assembled as maturated heterodimer (Lake et al., 2009). The NICD acts as a transcription factor that is released after ligand binding triggers its cleavage. It contains a nuclear localization sequence (NLS) that mediates its translocation to the nucleus, where it forms a transcriptional complex along with several other transcription factors. Once in the nucleus, several ankyrin repeats (ANK) and the RAM domain interacts with the NICD and CSL (CBF1, Suppressor of Hairless, Lag-1) proteins to form a transcriptional activation complex (Tamura et al., 1995). In humans, an additional

proline, glutamic acid, serine, threonine-rich (PEST) domain plays a role in NICD degradation (Weng et. al., 1995) (Figure 2).

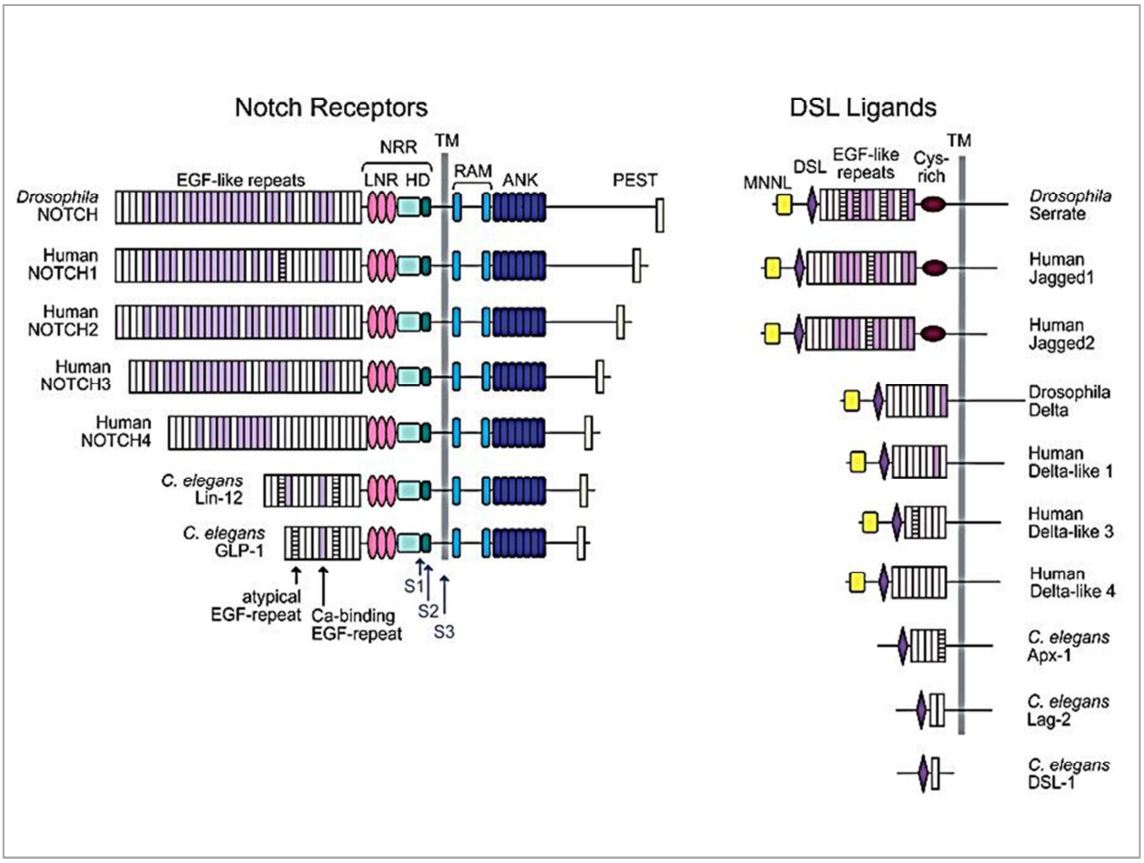

Figure 2: Notch receptors and ligands are evolutionarily conserved in Human, Fly and Worm

Notch Ligands are also type 1 single pass transmembrane proteins fall into the Delta/Serrate/Lag-2 (DSL) family of proteins which is named after the three canonical Notch ligands (Artavanis-Tsakonas, 1995; Kopan & Ilagan, 2009). Delta and Serrate are found in *Drosophila*, while Lag-2 is found in *C. elegans*. Human contain 3 Delta homologs, Delta-like 1, 3, and 4, as well as two Serrate homologs, Jagged 1 and 2. They contain a relatively short intracellular domain and large extracellular domain that contain one or more EGF motifs and a N-terminal DSL motif (Figure 2).

The core cellular events that lead to activation of the Notch signal pathway have been unraveled through extensive genetic, cell biological and biochemical studies using *Drosophila melanogaster*, *C elegans* and vertebrate model organisms (Artavanis-Tsakonas, 1995, 1999; Bray, 2006; Kopan & Ilagan, 2009) (Figure 1). Upon the binding of either type of ligands to Notch, the extracellular domain of Notch is mechanically pulled by the bound ligand that is internalized by endocytosis into the neighboring cell (Gordon et al., 2008). This pulling force induces a conformational change in the NRR domain, which makes this domain susceptible to the proteolytic cleaved at another site (S2 site) within this domain by a family of a disintegrin and metalloproteinase (ADAM) (Brou et al., 2000). Consequently, Notch lacking the most part of extracellular domain (NEXT) is formed and internalized by endocytosis (Brou et al., 2000). During the course of endocytosis, NEXT is further cleaved with the transmembrane domain (S3 site) by γ-secretase, leading to the liberation of the NICD from the plasma membrane (Struhl and Greenwald, 1999). Then, NICD is translocated into nucleus where it forms complex with CSL(CBF1, Suppressor of Hairless, Lag-1) transcription factor, and a Mastermind coactivator on the cis-regulatory sequences of the target gene enhancers (Gordon et al., 2008; Kovall & Blacklow et al., 2010; Yuan et al., 2016). This complex further recruits additional coactivators such as p300 to trigger chromatin remodeling to activate the transcription of the Notch target genes (Fryer, 2004; Kovall et al., 2017). It is important to note that each step of Notch signaling cascade is tightly regulated by various genes and cellular mechanisms to fine-tune signal output in a context specific manner (Guruharsha et al., 2012). For example, vesicle trafficking events such as exocytosis, endocytosis, and recycling can activate or inhibit Notch signaling in a cell and tissue specific manner, primarily because receptors,

ligands and key proteases required for signal activation are all membrane bound proteins (Yamamoto et al., 2010; Baron, 2012). Although numerous genetic screens have been performed to identify Notch signaling regulators in the past several decades using *Drosophila melanogaster*, *C elegans* and vertebrate model organisms and many new genes that affect this pathway have been identified, the field still lacks a comprehensive understanding of how Notch signaling pathway is fine-tuned, primarily due to lack of understanding of molecular functions of those genes (Artavanis-Tsakonas, 1995, 1999; Bray, 2006; Kopan & Ilagan, 2009) (Figure 3).

Component Function	Type	*Drosophila*	*Caenorhabditis elegans*	Mammals
Receptor		Notch	LIN-12, GLP-1	Notch 1–4
Ligand	DSL/DOS	Delta, Serrate		Dll1, Jagged1 and 2
	DSL only		APX-1, LAG-2, ARG-2, DSL1–7	Dll3 and 4
	DOS Coligands		DOS1–3, OSM7 and 11	DLK-1, DLK-2/EGFL9
	Noncanonical			DNER, MAGP-1 and -2, F3/ Contactin1, NB-3/Contactin6
Nuclear Effectors	CSL DNA-binding transcription factor	Su(H)	LAG-1	RBPjκ/CBF-1
	Transcriptional Coactivator	Mastermind	LAG-3	MAML1-3
	Transcriptional Corepressors	Hairless, SMRTR		Mint/Sharp/SPEN, NCoR/ SMRT, KyoT2
Receptor Proteolysis	Furin convertase (site 1 cleavage)	?	?	PC5/6, Furin
	Metalloprotease (site 2 cleavage)	Kuzbanian, Kuzbanian-like, TACE	SUP-17/Kuzbanian, ADM-4/TACE	ADAM10/Kuzbanian, ADAM17/TACE
	γ-secretase (site 3/site 4 cleavage)	Presenilin, Nicastrin, APH-1, PEN-2	SEL-12, APH-1, APH-2, PEN-2	Presenilin 1 and 2, Nicastrin, APH-1a-c, PEN-2
Glycosyltransferase modifiers	O-fucosyl-transferase	OFUT-1	OFUT-1	POFUT-1
	O-glucosyl-transferase	RUMI		
	β1,3-GlcNAc-transferase	Fringe		Lunatic, Manic, and Radical Fringe
Endosomal Sorting/ Membrane Trafficking Regulators	Ring Finger E3 Ubiquitin ligase (ligand endocytosis)	Mindbomb 1–2, Neuralized		Mindbomb, Skeletrophin, Neuralized 1–2
	Ring Finger E3 Ubiquitin ligase (receptor endocytosis)	Deltex		Deltex 1–4
	HECT Domain E3 Ubiquitin ligase (receptor endocytosis)	Nedd4, Su(Dx)	WWP-1	Nedd4, Itch/AIP4
	Negative regulator	Numb		Numb, Numb-like, ACBD3
	Neuralized Inhibitors	Bearded, Tom, M4		
	Other endocytic modifiers	sanpodo		
NICD Degradation	F-Box Ubiquitin ligase	Archipelago	SEL-10	Fbw-7/SEL-10
Canonical Target bHLH Repressor Genes		*E(spl)*	*REF-1*	*HES/ESR/HEY*

Kopan and Ilagan, 2009

Figure 3: Core components and modifiers of the Notch signaling pathway

In *Drosophila*, extensive genetic studies identified many genes encoding components of Notch signaling. Such pioneer works provided a framework to elucidate the mechanisms of Notch signaling (Artavanis-Tsakonas et al., 1999). However, although their contributions to the Notch signaling pathway have been perceived by such genetic studies, biochemical and cellular functions of proteins encoded by such genes, including *almondex* (*amx*) remains unclear (Schweisguth, 2004). *Drosophila almondex* (*amx*) gene has been known to encode a positive regulator of Notch signaling for the past ~40 years but its precise molecular function has been obscure.

The first *amx* allele (amx^1) was described as an X-linked female sterile mutation that exhibited slightly reduced and narrowed shaped eyes that resembled the shape of an almond (Lindsley & Grell, 1968). The early amx^1 allele was characterized predominantly as a maternal effect gene (Shannon, 1973). A maternal effect is a situation where the phenotype of an organism is determined not only by the environment it experiences and its genotype, but also by the environment and genotype of its mother (Figure 4). In genetics, maternal effects occur when an organism shows the phenotype expected from the genotype of the mother, irrespective of its own genotype, often due to the mother supplying messenger RNA or proteins to the egg. It has been proposed that maternal effects are important for the evolution of adaptive responses to environmental heterogeneity.

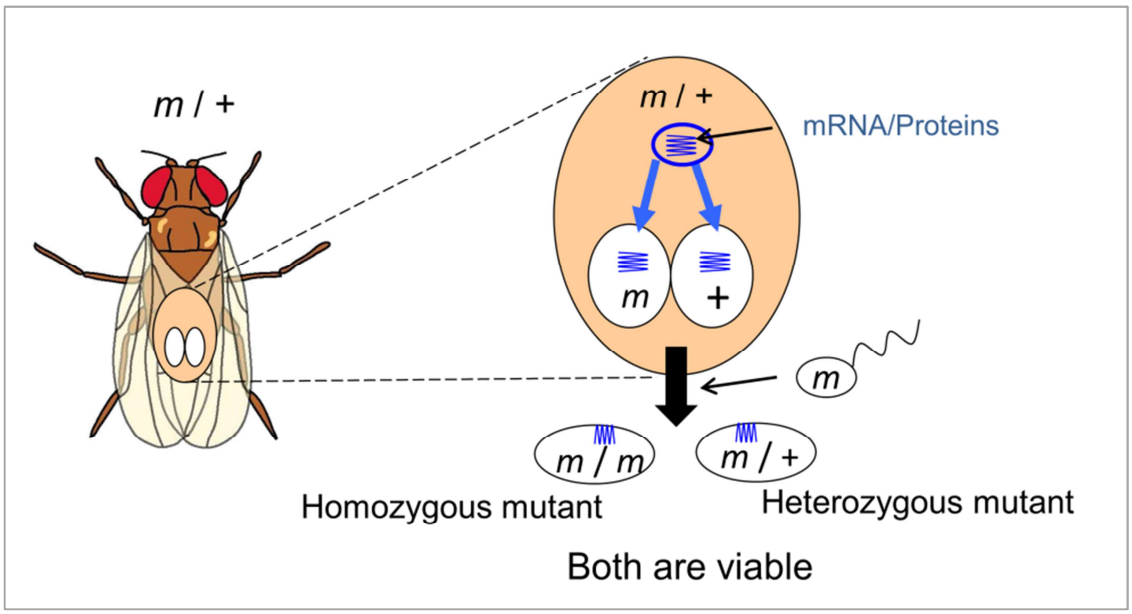

Figure 4: Maternal effect gene

amx was characterized as maternal effect gene because fertilized eggs obtained from amx^{1} homozygous or hemizygous (amx^{1}/deficiency) females fail to hatch out of their egg shell (Shannon, 1972, 1973; Perrimon et al., 1986). These embryos that failed to hatch show a strong neurogenic phenotype, a neural hyperplasia at the expense of epidermis, in the neuroectoderm (Lehmann et al., 1981, 1983; Michellod et al., 2003). This phenotype is characteristic for mutants that show strong Notch signaling defects during early embryogenesis, because Notch signaling activity is required for lateral inhibition during neuroblast segregation (Poulson, 1939, 1940) (Figure 5).

Early neurogenesis in *Drosophila* is controlled by two groups of interrelated genes. First, expression of the proneural genes establishes neurocompetence of the cells forming the proneural clusters within the neuroectoderm (Simpson and Carteret, 1990; Skeath and Carroll, 1994). Next, the neurogenic genes provide a regulatory signal for

neurocompetence through a cell-to-cell interaction mechanism, called lateral inhibition. Lateral inhibition among cells of the proneural cluster leads to election of a single neuroblast and repression of neurocompetence in the neighboring cells, resulting in their commitment towards an epidermal fate. Loss of function of the embryonic neurogenic genes results in neural commitment of all cells of the proneural clusters; indeed, no lateral inhibition occurs and epidermoblasts are thus not specified. The embryonic neurogenic phenotype corresponds to a hyperplasia of the central nervous system (CNS) at the expense of the epidermis (Lehmann et al., 1983) (Figure 5).

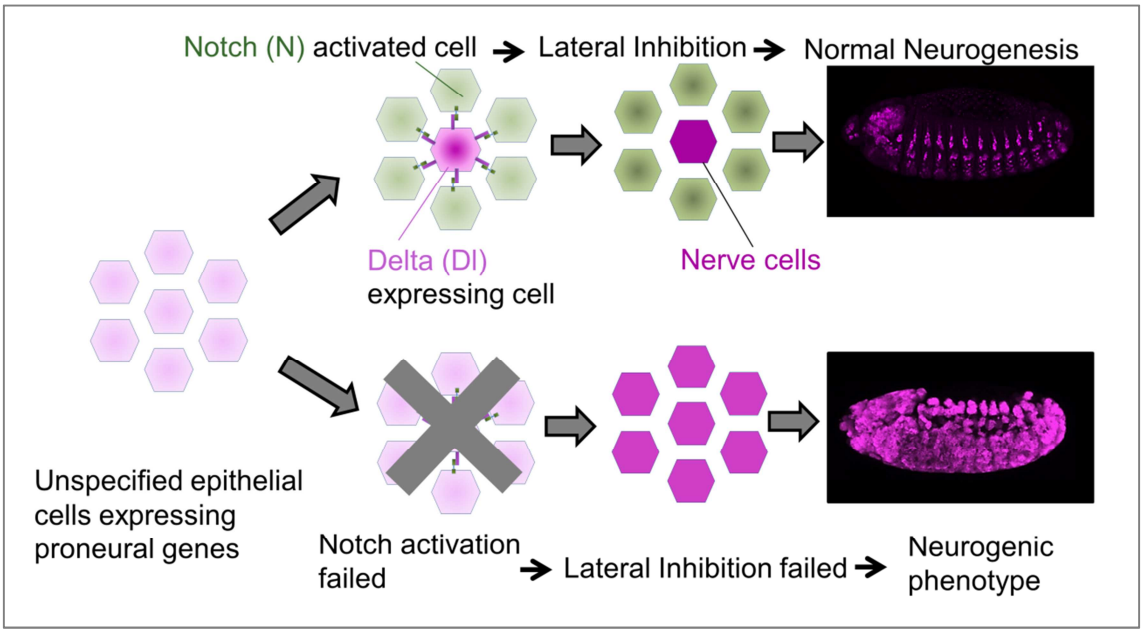

Figure 5: Notch involvement in cell fate decision through lateral inhibition during *Drosophila* neurogenesis

In *Drosophila*, seven embryonic neurogenic genes were initially identified: *Notch (N), big brain (bib), mastermind (mam), neuralized (neu), Delta (Dl), Enhancer of split (E(spl)*), and *almondex (amx*) (Figure 6). Genetic studies based on epistatic

interactions between *amx* and other neurogenic genes in embryos suggested that *amx* acts upstream of the network formed by these genes (de la Concha *et al.*, 1988). However, its precise molecular function has been obscure for long time.

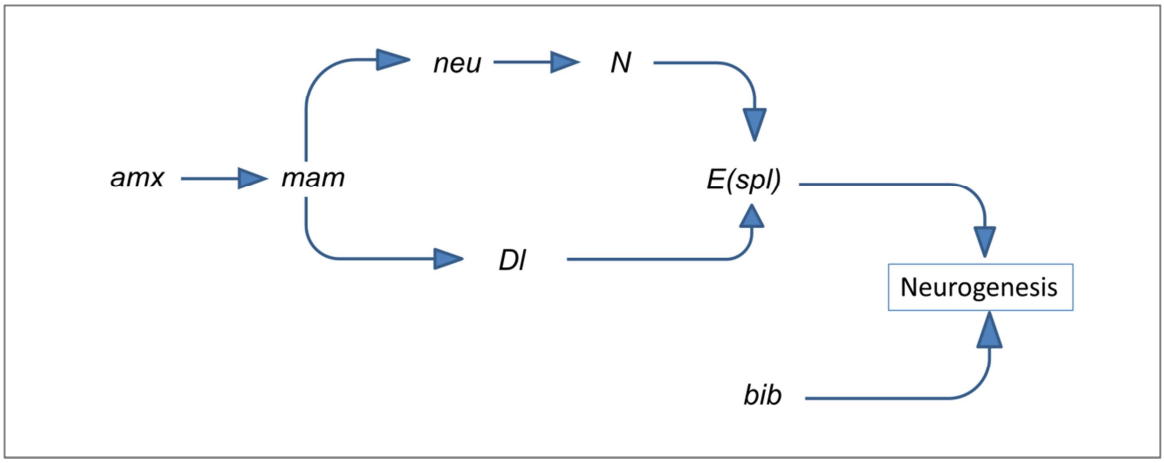

Figure 6: Historically, seven neurogenic genes were identified in *Drosophila*, in where it was suggested that *amx* acts upstream of the network formed by these genes

Epistasis analysis involving amx^{1} and the overexpression of various forms of *Notch* suggested that Amx acts at the level of Notch cleavage by γ-secretase (Michellod & Randsholt, 2008). In addition, the same group proposed that *amx* is also required for Notch signaling during development of the wing imaginal disc, based on the observation that amx^{m} flies with the maternal contribution of *amx* have notched wings (Michellod et al., 2003). Therefore, it was suggested that, the amx^{1} allele, which carries a premature termination codon removing the 1/3 of the deduced Amx C-terminal fragment, is a hypomorphic allele, because amx^{1} homozygous flies with the maternal contribution did not show the Notched wing (Michellod & Randsholt, 2008). However, considering that amx^{m} is a complicated allele generated by combination of a deletion

and duplication involving *amx* and neighboring genes (e.g. *Dsor1*), it is difficult to evaluate, what phenotypes are caused by loss of *amx* and what do so by other genes.

LaBonne and Mahowald (1985) previously shown that the maternal neurogenic phenotype associated with *amx* mutation was rescued by the transplantation of ooplasm from wild-type. However, for the efficient recuse, the wild-type ooplasm needs to be injected not after stage 3, although the first defect of neurogenesis was observed only at stage 9 (LaBonne & Mahowald, 1985) (Figure 7). Thus, I speculated that potential defects of the Notch signaling pathway could be observed before the initiation of neurogenesis in *Drosophila* embryo.

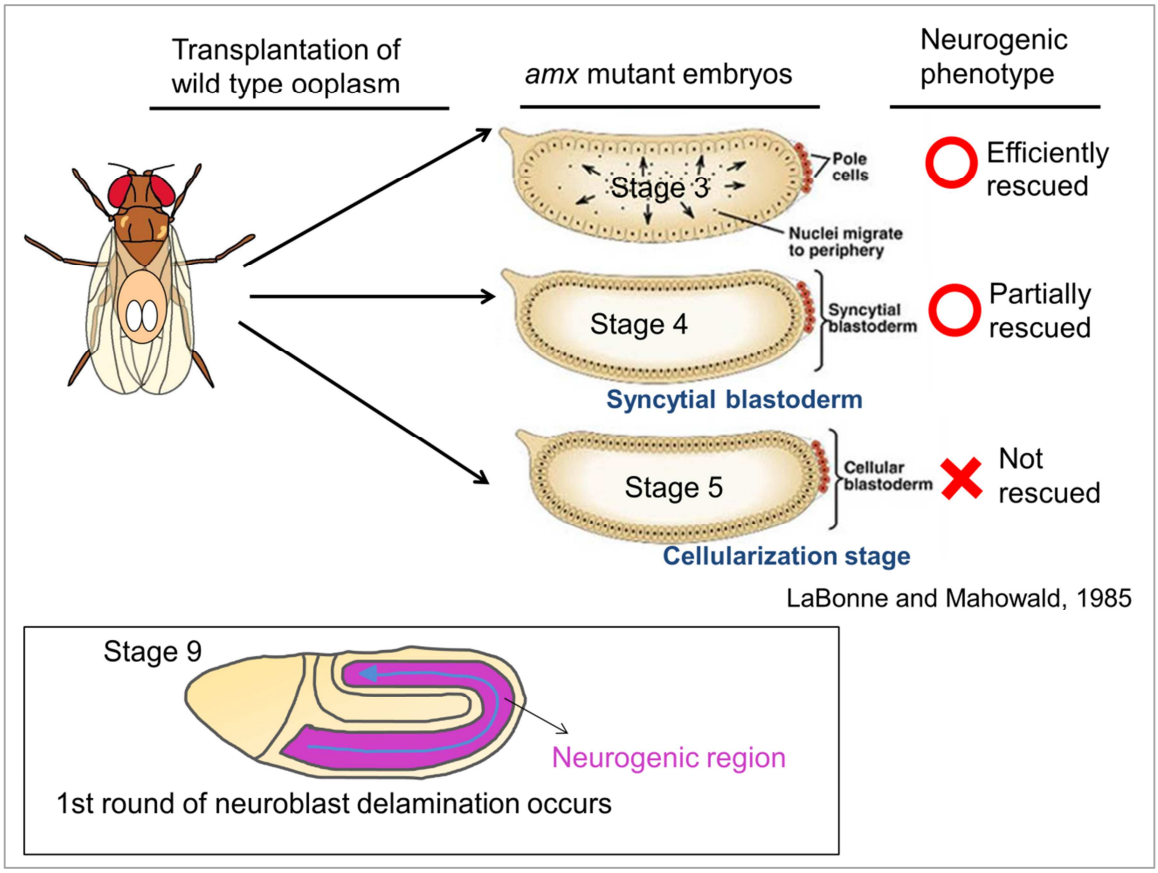

Figure 7: *amx* mutant phenotype was rescued by the transplantation of ooplasm from wild-type before stage 3

amx and its paralogs are evolutionarily conserved between *Drosophila* to human (Michellod & Randsholt, 2008). The *amx* family genes encode a predicted transmembrane protein with a C-type Lectin domain and a DRF motif, conserved in G-protein coupled receptor (Michellod & Randsholt, 2008). Recently, TM2D3, the human homolog of *amx*, was identified as a late-onset Alzheimer's disease associated gene, whose mutation was found to associate with the increased risk of this disease (Jakobsdottir et al., 2016). Alzheimer's disease is characterized by the plaques of β-amyloid, which is produced from β-amyloid precursor protein by the cleavage of γ-secretase. Therefore, it was proposed that Amx/TM2D3 may contribute directly or indirectly to the γ-secretase cleavage of Notch and β-amyloid precursor protein (Jakobsdottir et al., 2016). However, molecular nature of such potential interaction between Amx/TM2D3 and γ-secretase remains unclear.

In this study, I took advantage of the newly generated clean null allele of *amx* using CRISPR-mediated homology directed repair to understand the role of *amx* during the early embryogenesis (Li-Kroeger et al., 2018). While confirming earlier results that *amx* play critical roles in lateral inhibition during neuroectoderm development, I also found that *amx* is partially required for inductive signaling during mesoectoderm development. Close examination of subcellular distribution of Notch and its ligands revealed that maternally deposited *amx* is required for the normal distribution of Notch at stage 5 of embryogenesis. Although it still remains to be determined what effect such alterations in the distribution of Notch may have on activation of Notch signaling, I propose that Amx directly or indirectly regulates Notch trafficking, which potentially impacts on the signal activation during early embryogenesis.

2. Materials and methods

2.1 Drosophila stocks and crosses

All fly experiments were performed at 25°C on standard *Drosophila* culture media. Canton-S was used as a wild-type control strain. The genotypes of other *Drosophila* lines used were: $amx^{\Delta CDS,ywing2+}$, referred to as amx^{N} to indicate it is a *Null* allele of *amx* in this manuscript (Li-Kroeger et al., 2018); *Df(1)BSC663* (X:9,217,347...9,284,575), a molecularly defined deletion uncovering *amx* and other nearby genes generated by FLP/FRT mediated recombination (Parks et al., 2004); $pecanex^{3}$ (pcx^{3}), a loss-of-function allele of *pcx* (Mohler, 1977; Mohler & Carroll, 1984); *Protein disulfide isomerase* (*Pdi*)-*GFP* (a protein trap line of *Pdi*) (Kelso et al., 2004); a line carrying a ~3.3kb genomic rescue construct containing the wild-type *amx* inserted on to a second chromosome phiC31 docking site (VK37), referred to as *amx[+]*, (Jakobsdottir et al., 2016).

amx homozygous and hemizygous embryos lacking its maternal contribution (amx^{mz}) were obtained by the cross of amx^{N}/*Df(1)BSC663* females with amx^{N}/Y males (Figure 11, Figure 13, Figure 15, Figure 16, Figure 17, Figure 18, Figure 20, Figure 21, Figure 22, and Figure 23). *amx* homozygous and hemizygous embryos with its maternal contribution (amx^{z}) were obtained by the cross of amx^{N}/*FM7c.GFP* females with amx^{N}/Y males and negatively selected by staining with anti-GFP antibody (Figure 11). *amx* heterozygous embryos lacking its maternal contribution ($amx/+^{m}$) were obtained by the cross of amx^{N}/amx^{N} females with *FM7c.GFP*/Y males and positively selected by staining with anti-GFP antibody (Figure 11). *amx* hemizygous embryos lacking its maternal contribution (amx/Y^{m}) were obtained by the cross of amx^{N}/amx^{N}

females with *FM7c.GFP/Y* males and negatively selected by staining with anti-GFP antibody (Figure 11). *pcx* homozygous and hemizygous embryos lacking its maternal contribution (pcx^{mz}) were obtained by the crossing of pcx^{3}/pcx^{3} females with pcx^{3}/Y males (Figure 19). *amx*/Y embryos, which were negatively selected by staining with anti-Sex lethal antibody, lacking its maternal contribution and carrying *Pdi-GFP* were obtained by the cross of amx^{N}/amx^{N} females with +/Y; *Pdi-GFP/TM3* males (Figure 23). To perform rescue experiments, I generated a strain (amx^{N}; *amx[+]*), in which amx^{N} is rescued by the genomic rescue construct of *amx* (Jakobsdottir et al., 2016). In this strain, *amx* homozygous and hemizygous embryos do not express *amx* from its endogenous loci but were supported by the exogenous transgene of *amx* (Figure 11, Figure 13, and Figure 18).

2.2 Generation of an amx null mutant, amx^{N}, by CRISPR mediated homology directed repair

The amx^{N}, a null mutant of *amx*, used in this study was reported before (Li-Kroeger et al., 2018). In brief, we designed two guide RNAs (gRNAs) that targets 5' and 3' of the *amx* coding sequence (CDS), and deleted the *amx* CDS by replacing it with a $yellow^{wing2+}$ marker using CRISPR mediated homology directed repair. The amx^{N} allele was genetically followed based on the $yellow^{wing2+}$ marker in a *yellow*-background. Successful gene replacement event was validated with PCR. The female sterility and maternal effect neurogenic phenotype was fully rescued by a genomic rescue construct of *amx* reported before (Jakobsdottir et al, 2016). The primers were used to amplify both homology arms as follows: upstream-fwd: ctctctGGTCTCtGACCgagtgctccctgctaaaaccatgc; upstream-rev:

agagagGGTCTCgATCCggaatagcaagatcttctcaaaaacgtgtac; downstream-fwd: ctctctGGTCTCtTTCCcattggccgctttagtcgtaggag; downstream-rev: agagagGGTCTCgTATAgagagagtacctgctctttcactcc. The single-guide RNAs (sgRNAs) were used to cut the *amx* coding sequence out as follows: upstream sense gRNA-gtcGAAGATCTTGCTATTCCTAA; upstream antisense gRNA-aaacTTAGGAATAGCAAGATCTT; downstream sense gRNA-gtcgTCCATTTAAGTTGTGACCAT; downstream antisense gRNA-aaacATGGTCACAACTTAAATGGA. sgRNAs were cloned into pAct-Cas9 (Addgene plasmid #62209).

2.3 Immunostaining

The antibody staining of embryos was performed as previously described (Rhyu et al., 1994). Briefly, embryos were collected using yeast paste coated agar slide and dechorionated in 50% bleaching solution (haiter, Kao). The dechorionated embryos were fixed by using mixture of Haptane and 4% Paraformaldehyde/PBS (1:1) for 30 min. After fixation, the vitelline membrane of the embryos was removed by using mixture of Haptane and 100% Methanol (1:1). After that washed with 100% Methanol and preserved at -20 °C for later use.

The primary antibodies used were: rat anti-Elav (7E8A10, 1:500) (O'Neill et al., 1994); mouse anti-Notch intracellular domain (C17.9C6, 1:100) (Fehon et al., 1990); mouse anti-Delta extracellular domain (C594.9B, 1:100) (Artavanis-Tsakonas, 1996); guinea pig anti-Myosin II (MyoII) (1:100) (see below); mouse anti-Sec5 (22A2, 1:50) (Murthy et al., 2003); guinea pig anti-Hrs (1:400) (Lloyd et al., 2002); rabbit anti-Rab7

(1:5,000) (Tanaka & Nakamura, 2008); rabbit anti-Rab11 (1:10,000) (Tanaka & Nakamura, 2008); mouse anti-Sex-lethal (M18, 1:20) (Bopp et al., 1991); rabbit anti-GM130 (Ab30637, 1:100, Abcam) (O'Sullivan et al., 2012); Biotinylated Peanut Agglutinin (PNA) (B-1075-5, 1:100, Vector Laboratories) (Yano et al., 2005); rabbit anti-GFP (598, 1:500, MBL) (Suzuki et al., 2010).

The fluorescent secondary antibodies used were: Alexa488-conjugated donkey anti-rat (Jackson ImmunoResearch); Cy3-conjugated donkey anti-mouse (Jackson ImmunoResearch), Alexa488-conjugated goat anti-guinea pig (Invitrogen); Alexa488-conjugated donkey anti-rabbit (Jackson ImmunoResearch); Streptavidin Alexa Fluor 555 conjugate (Invitrogen); Alexa488-conjugated goat anti-mouse (Molecular Probes); and Alexa Flour 488 donkey anti-Rabbit (Jackson ImmunoResearch). All of these secondary antibodies were used at 1:500 dilution.

For F-Actin staining embryos were collected using yeast paste coated agar slide and dechorionated in 50% bleaching solution (haiter, Kao). The dechorionated embryos were fixed by using mixture of Haptane and 8% Paraformaldehyde/PBS (1:1) for 30 min. After fixation, the vitelline membrane of the embryos was removed manually by using hand and after that, immediately used for staining. F-Actin was visualized using Alexa Flour-488 phalliodin (Molecular Probes) for 1 hr.

Confocal microscopy images were collected using LSM 700 (Zeiss), and super resolution images were taken by LSM 880 with AiryScan FAST (Zeiss). Confocal microscopic images corresponding the ventral-lateral region were obtained until 30 µm

depth from the apical surface, and Z sections were constructed from them (Figure 15, Figure 17, Figure 18, Figure 19, and Figure 20). Higher magnification images of X-Y focal planes were taken at 2 µm from the apical surface (Figure 17, Figure 21, Figure 22, and Figure 23). Images were analyzed by LSM Image Browser ZEN 2012 (Zeiss).

2.4 Anti-Myosin II antibody generation

A synthetic peptide of 15 amino acids (SSRLTGTPSSKRAGG) corresponding to the 2022nd to 2036th amino acids of Myosin heavy chain, non-muscle Myosin II (MyoII) (*zipper*) of *Drosophila* was injected to Guinea pigs for polyclonal antisera production using a standard protocol (Cooper & Paterson, 1995).

2.5 In situ hybridization

In situ hybridization of embryos was performed as described previously (Takashima & Murakami, 2001). Antisense and sense RNA probes of *single-minded* (*sim*) were prepared as previously reported (Yamakawa et al., 2012). Briefly, antisense and sense probes labeled with Digoxigenin were generated from the cDNA clone of *sim*, using DIG RNA labeling mix (Roche), according to the manufactures' instructions. Hybridization was done at 59 °C for 15 hrs in a buffer containing 50% formamide, 5x SSC (750 mM NaCl, 75mM sodium citrate, pH 5.0), 50 µg/mL denatured salmon sperm DNA, and 0.1% Tween 20. Washed, treatment with mouse anti-DIG antibody (Roche), and histochemical staining was done. Images were obtained with the differential interference microscope (Axioskop 2 Plus, Carl Zeiss) and processed by WinROOF 2015 (Mitani Corporation).

2.6 Protein modeling

To model the potential protein structure of Amx, I utilized the *Phyre*[2] (Protein Homology/analogY Recognition Engine V 2.0) tool (http://www.sbg.bio.ic.ac.uk/phyre2) in intensive mode (Kelley et al., 2015).

2.7 Double blind test

Double blind test was performed by mixing 50 images of wild-type and mutant embryos of different stages and scored for subcellular Notch distribution by me and another lab. member.

3. Results

3.1 A null mutant allele of Drosophila amx, amx^{N}, shows maternal, but not zygotic neurogenic phenotype

The *Drosophila melanogaster* Amx protein is composed of 284 amino acid residues (Michellod & Randsholt, 2008). Although some earlier studies have depicted Amx as a three-pass transmembrane protein (Michellod & Randsholt, 2008), sequence analysis using more recent protein domain identification tools and homology comparison with orthologous genes in other species predict that Amx is a two-pass transmembrane domain protein with an N-terminal signal peptide (Jakobsdottir et al., 2016). Because there are no structural analysis performed on Amx and its orthologous proteins, I attempted to model this structure using the *Phyre2* tool (Software: Kelley et al., 2015) (Figure 8). This program also showed that Amx is likely to be a two transmembrane domain [designated as TM-helix 1 (orange) and TM-helix 2 (red)] protein with an N-terminal α-helix (blue) (Figure 8A). Based on this model, *Drosophila*

Amx has a signal peptide, which is likely to be cleaved off in the mature protein, followed by a stretch of amino acids that are rich in cysteine (Cys-rich region, green) (Figure 8B). This is followed by a C-Type Lectin like Domain (CTLD, yellow), TM1, a short intracellular loop containing an evolutionarily conserved DRF (Aspartic Acid-Arginine-Phenylalanine, orange star) motif, TM2, and a short extracellular/luminal tail (Figure 8B). Although several functional studies on *amx* and its orthologous *TM2D3* gene indicated the potential roles of the intracellular DRF motif and CTLD in their functions, the molecular role of these proteins have not been established yet (Michellod & Randsholt, 2008; Jakobsdottir et al., 2016).

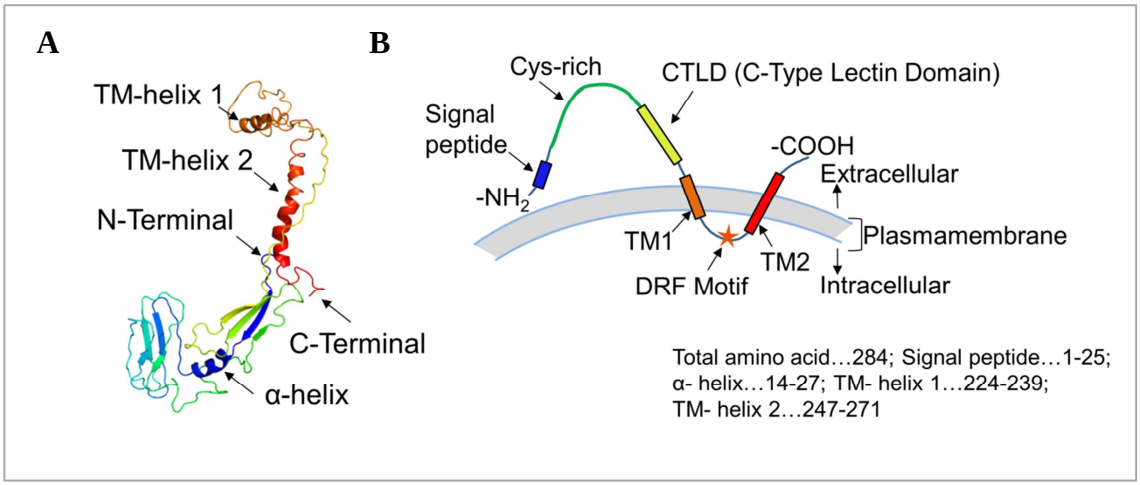

Figure 8: *amx* encodes a double-pass transmembrane protein. (A) Predicted 3D model by *Phyre2* showing two transmembrane (TM) domains, TM-helix 1(orange) and TM-helix 2 (Red) located in C-terminal, and an α-helix in N-terminal (blue). (B) Predicted topography by *Phyre2* showing that Amx is presumably a double-pass transmembrane protein comprises of TM1 (orange box) and TM2 (Red box) in C-terminal and a signal peptide (blue box) in N-terminal. Two conserved domains, a Cys-rich domain (green line) and C-Type Lectin Domain (CTLD; yellow box), are predicted in the extracellular domain. Another highly conserved DRF motif is predicted between TM1 and TM2 in the intracellular domain.

Most studies on *amx* have been performed using a single allele which is referred to as amx^{1} (Shannon, 1972, 1973; Lehmann et al., 1981, 1983; Perrimon et al., 1986; Michellod et al., 2003, Michellod & Randsholt, 2008). amx^{1} carries a 8 nucleotide deletion that introduces a premature stop codon after the 184th amino acid residue (Michellod & Randsholt, 2008) (Figure 9A). Thus, it is likely that amx^{1} generates a mutant protein that lacks the CTLD and following domains (Michellod & Randsholt, 2008). Previous studies showed that embryos homozygous or heterozygous for amx^{1} obtained from amx^{1} homozygous females (no maternal *amx* provided to the offspring) exhibit strong neurogenic phenotypes, while amx^{1} homozygote and hemizygous animals derived from amx^{1} heterozygous mothers (maternal *amx* provided to the offspring) are viable and do not exhibit any phenotypes (Shannon, 1972, 1973). amx^{1} mutant has been described as a hypomorphic (partial loss of function) allele in previous studies (Lehmann et al., 1981, 1983; Michellod et al., 2003), while others have described it as an amorphic (null) allele (de la Concha et al., 1988). To overcome the issue of different interpretation regarding allelic strengths, a null allele of *amx* by taking a deletion that encompasses *amx* and its neighbouring *Dsor1* gene and reintroducing *Dsor1* through a genomic rescue construct (referred to as amx^{m}) has been generated (Michellod et al., 2003). This study confirmed that *amx* is indeed required maternally for proper Notch signalling during embryogenesis and also revealed that it is required zygotically for wing development, since the amx^{m} zygotic mutants exhibited a wing Notching phenotype (Michellod et al., 2003). Such wing phenotype was not reported in amx^{1} mutant, which led to a conclusion that amx^{1} is a hypomorphic allele (Lehmann et al., 1981, 1983; Michellod et al., 2003). However, a deletion (*Df(1)FF8*) used in that study has not been molecularly defined (Michellod et al., 2003). In addition, rescue

experiments have not been performed to assess whether the observed phenotypes are due to loss of *amx* mutation. Therefore, it is still unclear whether *amx* is truly a maternal effect gene or has zygotic requirements in Notch signaling.

To address those questions, in collaboration with Dr. Yamamoto, we generated a clean null allele of *amx* referred to as amx^{N} (Figure 9B). This allele was generated via CRISPR mediated homology directed repair and introduced a ~2.9-kb cassette of y^{wing2+} as a dominant marker (Li-Kroeger et al., 2018).

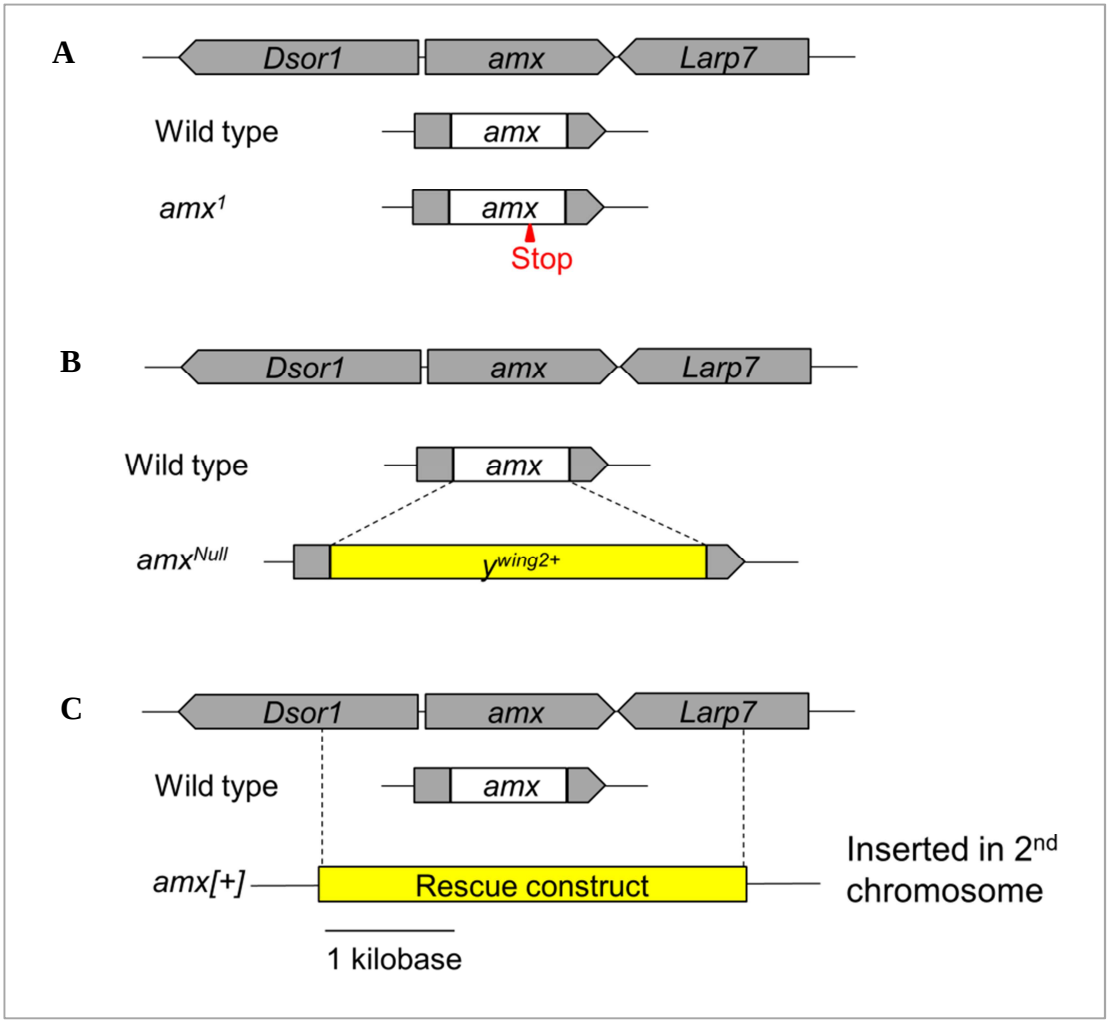

Figure 9: The schematic diagrams showing genomic structure of amx^{1} (A) and amx^{Null} (B) and *amx[+]* (C) genome.

I found that amx^{N}/Y hemizygous male flies that are derived from amx^{N}/+ females are viable, fertile and do not exhibit any obvious morphological defects in eye, wing, and notum, similar to amx^{1} alleles (Shannon, 1972, 1973) (Figure 10). However, amx^{N}/amx^{N} homozygous female flies derived from amx^{N}/+ females were sterile, although they were viable and did not show obvious morphological defects in eye, wing, and notum, similar to amx^{1} alleles (Shannon, 1972, 1973) (data not shown). This sterility was fully suppressed by introducing a genomic rescue construct *amx[+]*, that only contains the full coding sequence for *amx* but not neighbouring genes, demonstrating that this defect is attributed to the loss of *amx* functions (Jakobsdottir et al., 2016) (Figure 9C). Based on these experiments, I conclude that *amx* is not required in the Notch signaling zygotically, suggesting that the wing Notching phenotype reported earlier in amx^{m} animals are caused by defects in other genes (Michellod et al., 2003).

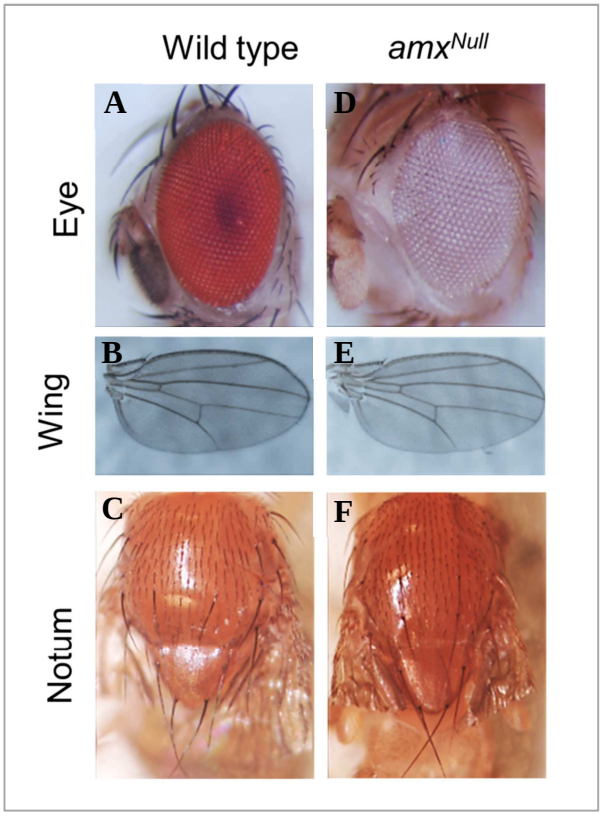

Figure 10: (A-F) Adult phenotypes of wild-type (A-C) and amx^{Z} males (D-F). The pictures of eyes (A, D), wings (B, E), and nota (C, F).

Using the *amx*^{N} allele, I next analysed the nature of neurogenic phenotype in embryos associated with the null condition of *amx*. To exclude potential embryonic phenotypes that may be associated with background mutations in *amx*^{N}, I assessed the phenotypes of embryos obtained from genetic crosses between trans-heterozygote females of *amx*^{N} and *Df(1)BSC663*, a small deficiency uncovering *amx* locus, and *amx*^{N}*/Y* males. The embryos resulting from this cross include *amx*^{N} homozygote females, *amx*^{N}/*Df(1)BSC663* females, *amx*^{N}/Y males, and *Df(1)BSC663*/Y males, all of which are homozygote or hemizygote of *amx* and lack of the maternal contribution of *amx*. In this study, I refer these to as *amx*^{mz} embryos, because they are considered as maternal (m) and zygotic (z) null alleles of *amx*. As reported previously using *amx*^{1} allele, I found that the *amx*^{mz} embryos showed neurogenic phenotype in all cases examined, based on the neural hyperplasia detected by anti-Elav antibody (neuron-specific) staining (Figure 11B, n=20) compared with wild-type embryos (Figure 11A, n=20) (Jakobsdottir et al., 2016). I confirmed that the neurogenic phenotype of *amx*^{N} homozygote and hemizygote without *amx* maternal contribution was rescued by introducing a genomic fragment encompassing wild-type *amx* locus (*amx[+]*) into their mothers, demonstrating the specificity of this phenotype (Figure 11C, n=35).

In previous studies, it was shown that *amx*^{1} homozygote or hemizygote with maternal contribution of *amx* (produced from *amx*^{1}/+ heterozygous mothers) did not show any neurogenic phenotype, which was the basis of classifying *amx* as a maternal but not a zygotic neurogenic gene (Shannon, 1973; Michellod et al., 2003). However, it is possible that the potential zygotic neurogenic phenotype may be suppressed, if *amx*^{1} is indeed a hypomorphic allele (Lehmann et al., 1981, 1983; Michellod et al., 2003).

However, my analyses showed that embryos of *amx*^{N} homozygote and hemizygote with its maternal contribution (*amx*^{z}) showed normal nervous system in all cases examined, confirming the idea that *amx* is indeed required maternally but not zygotically for proper neurogenesis (Figure 11D, n=24).

Previously, it was shown that maternal neurogenic phenotype associated with *amx*^{m} can be suppressed by a paternal wild-type *amx* gene in a small fraction of the animals (7%) (Michellod et al., 2003). Because this conclusion was made based on observation of the rescue of the cuticle phenotype rather than directly examining the neurogenic defect; epidermal tissue that forms cuticle was not differentiated due to the failure of lateral inhibition promoting the differentiation of epidermoblasts instead of neuroblast, I decided to revisit this phenotype by performing neuronal staining of embryos obtained from *amx*^{N} homozygous females (*amx*^{N}/*amx*^{N}) crossed to wild-type males (+/Y). I found that the maternal neurogenic phenotype of *amx* was partially suppressed, because those *amx*^{N}/+ embryos showed weak neurogenic phenotypes (Figure 11E, n=33, 40%), which were not observed in *amx*^{mz} hemizygote embryos in all cases examined (Figure 11F, n=53). However, these embryos did not hatch suggesting that zygotic *amx* is not sufficient to supress the embryonic lethality caused by lack of maternal *amx* (data not shown). In conclusion, my analysis using a clean null mutant allele of *amx* confirmed that *amx* is a maternal but not zygotic neurogenic gene. In addition, consistent with previous reports, I observed that this maternal neurogenic phenotype can be partially suppressed by paternal introduction of a wild-type *amx* gene (Figure 11).

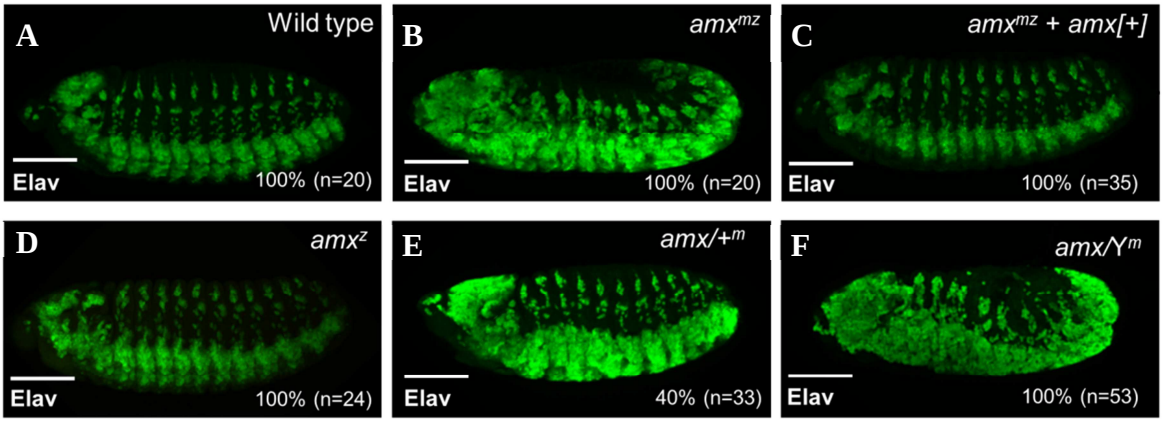

Figure 11: *amx* is a maternal but not zygotic neurogenic gene. **(A-F)** Embryos were stained with an anti-Elav (neuron-specific) antibody: wild-type (A), amx^{mz} (B), amx^{mz} rescued by *amx[+]* (amx^{mz} + *amx[+]*) (C), homozygous and hemizygous amx^{N} with its maternal contribution (amx^{z}) (D), heterozygous amx^{N} without its maternal contribution ($amx/+^{m}$) (E), and hemizygous amx^{N} without its maternal contribution (amx/Y^{m}) (F). Numbers at lower right show the percentage of embryos with the presented phenotype shown in the images for their genotype and the number of embryos examined (in parentheses). Scale bar: 100 μm.

3.2 amx is required for Notch signaling from very early stage of embryogenesis

LaBonne and Mahowald (1985) previously showed that the maternal neurogenic phenotype associated with *amx* can be rescued by the transplantation of ooplasm from wild-type oocytes into embryos obtained from amx^{1} mutant mothers. However, they reported that the wild-type ooplasm needs to be injected prior to stage 3 for efficient recuse (LaBonne & Mahowald, 1985) (Figure 7). Considering that the first defect in neurogenesis can only be observed after stage 9, I speculated that *amx* may play a role in Notch signaling before the initiation of neurogenesis in *Drosophila* embryo. Prior to the requirement in neuroblast segregation in the neuroectoderm, Notch signaling is required for the specification of mesoectodermal cells, which are formed as a single row

of cells adjacent to the mesoderm in each lateral half of an embryos at stage 6 (Morel & Schweisguth, 2000) (Figure 12). In these cells, Notch signaling is activated through the interaction with active Delta (Dl) ligand presented by the mesodermal cells, leading to the transcriptional activation of *single-minded* (*sim*) gene, a direct target of Notch signaling in stage 6 (Morel & Schweisguth, 2000). In stage 9, the two rows of cells expressing *sim* merged into a single row along the midline as a result of the gastrulation (Morel & Schweisguth, 2000).

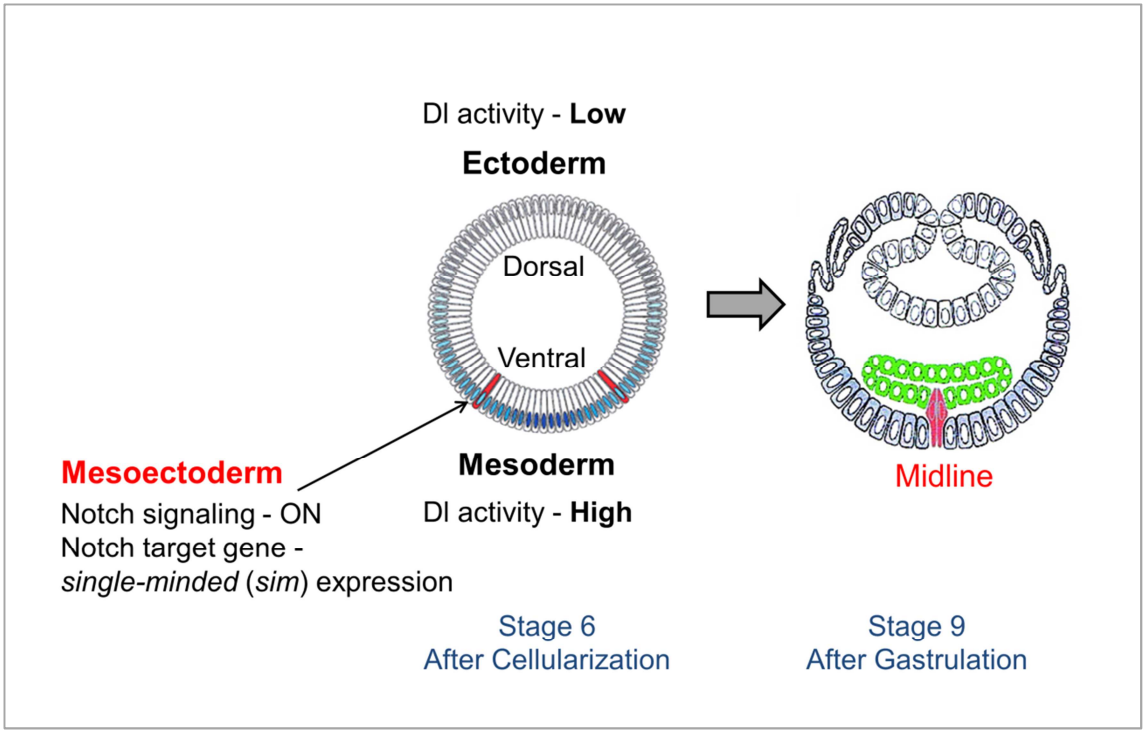

Figure 12: Notch signaling activation is spatially controlled in the mesoectoderm.

In stage 6 wild-type embryos, *sim* expression is detected by an anti-sense probe against *sim* in two rows of cells by *in situ* hybridization, as viewed from the ventral side of an embryo (Figure 13A, n=11) (Morel & Schweisguth, 2000). In stage 9 wild-type embryos, the two rows of cells expressing *sim* merged into a single row along the midline as a result of the gastrulation (Figure 13B, n=10) (Morel & Schweisguth, 2000). In contrast, in amx^{mz} embryos, I found that the rows of cells expressing *sim* was interrupted, and the signal of *in situ* hybridization was reduced at stage 6 in all cases examined (Figure 13C, n=8). At stage 9 of these embryos, the midline cells expressing *sim* was discontinuous, and the signal level of *sim* mRNA was also reduced in all cases examined (Figure 13D, n=15). Furthermore, the defects in *sim* expression in amx^{N}/Y males obtained from amx^{N} homozygote females can be restored if the mother carried a genomic rescue construct of *amx* (*amx[+]*), demonstrating that this phenotype is caused by maternal lack of *amx* (Figure 13E,F, n=10 for each). On the other hand, a sense probe against *sim* (control probe) did not show detectable signal at both stages in all examined wild-type embryos, demonstrating that the signal of *sim* expression was specific (Figure 13G,H, n=15 for each).

In various mutants of genes encoding the core components of Notch signaling, expression of *sim* has been reported to be completely abolished (Lecourtois & Schweisguth, 1995; Morel & Schweisguth, 2000). Considering that there is some residual expression of *sim* in amx^{mz} embryos, lack of *amx* likely diminishes but does not abolish Notch signaling in this context. Partial but not absolute requirement of a maternal Notch signaling gene in the mesoectoderm specification was also reported in *pecanex* (*pcx*) mutants (Yamakawa et el., 2012). Considering that both *pcx* and *amx*

maternal and zygotic mutants showed strong neurogenic phenotypes during neuroectoderm specification, it is possible that these genes play context specific roles in Notch signaling.

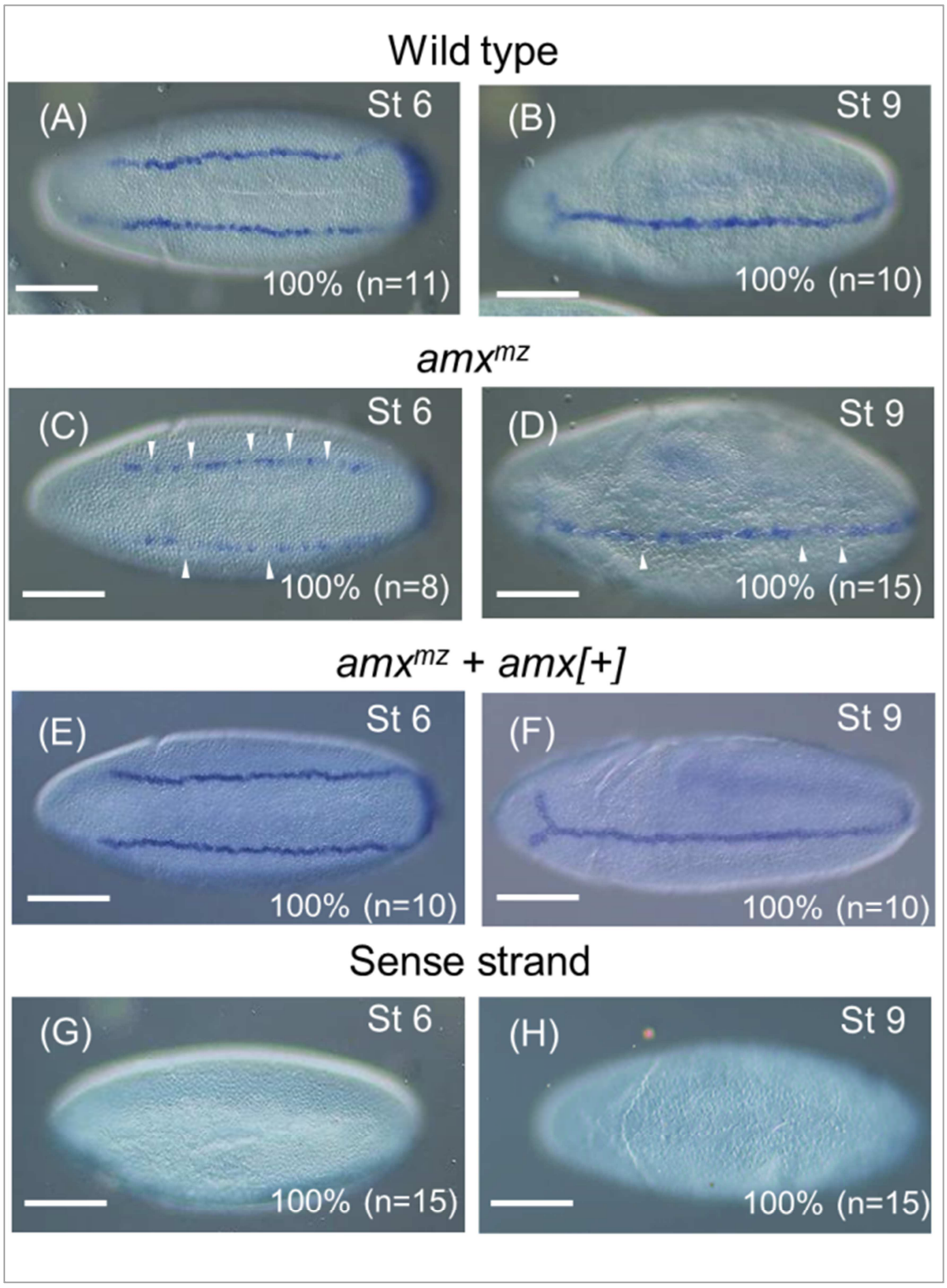

Figure 13: *amx* is required for Notch signaling from very early stage of embryogenesis. (A-F) *sim* expression detected by *in situ* hybridization using an anti-sense probe in wild-type (A, B), amx^{mz} (C, D), and amx^{mz} + *amx[+]* (E, F) embryos. At stage 6 (St 6) (A, C, E) and 9 (St 9) (B, D, F), *sim* expression was observed in two and one stripes of cells, respectively. Gapes of *sim* expression were indicated by white arrowheads in C and D. (G, H) Wild-type embryos probed by sense probe of *sim* (control probe) at stage 6 (St 6) (G) and 9 (St 9) (H). The percentages of embryos showing the presented phenotype are shown in the bottom right. The numbers of embryos examined (n) are shown in parentheses. Scale bar is 100 µm.

3.3 Subcellular distribution of Notch is altered in amx^{mz} embryos at stage 5

Our analyses above showed that Notch signaling activity was reduced in amx^{mz} embryos at stage 5. Michellod and Randsholt (2008) previously demonstrated that overexpression of *NICD* (Notch Intracellular Domain, a constitutively activated Notch that is independent of S3 cleavage) but not *NEXT* (Notch Extracellular Truncation, a form of constitutively activated Notch that is independent of ligands and S2 cleavage but is dependent on S3 cleavage) nor full-length Notch can partially suppress the failure of cuticle formation, which is due to the neural hyperplasia at the expense of epidermal cells, in amx^{1} homozygous embryos lacking the maternal contribution of *amx*. Based on this data, it was suggested that Amx may be involved in the γ-Secretase mediated S3 cleavage of Notch (Michellod & Randsholt, 2008). Considering that the S3 processing of Notch depends on the proper endocytic trafficking of Notch (Gupta-Rossi et al., 2004), I assessed whether intracellular distribution of Notch was affected in the amx^{mz} embryos at stage 5 when mesoectodermal cells begin to form.

During stage 5, syncytial blastoderm changes into cellular blastoderm through the cellularization (Figure 14A-C). At the early stage 5, the apical membrane of the syncytium is rich in microvilli that serves as a source of membrane to support the rapid invagination of the lateral plasma membrane (Figure 14A,B) (Figard et al., 2013, 2016). The microvilli gradually shrink during mid-stage 5, and eventually disappear as the invagination of the lateral plasma membrane is completed in late stage 5 embryos (Figure 14C) (Figard et al., 2013, 2016). These three sub-stages (early, mid, late) within stage 5 can be discriminated based on the position of the leading edge (tip) of the invaginating lateral plasma membrane (Figard et al., 2013, 2016). Because this tip is enriched in Myosin II (MyoII), immunostaining with an anti-MyoII antibody provides us a reference regarding these sub-stages (Figure 13) (He et al., 2016).

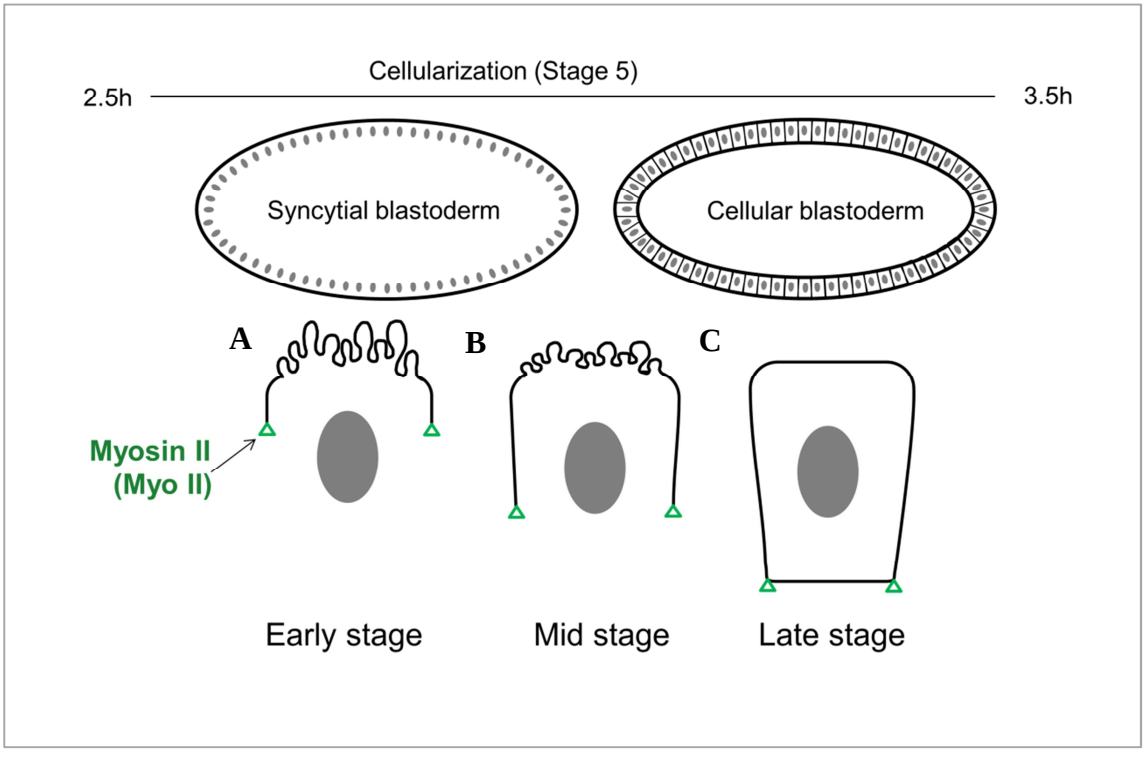

Figure 14: Cellularization stage during *Drosophila* early embryogenesis. (A-C) During cellularization process, syncytial blastoderm (upper left) changes into cellular

blastoderm (upper right), which can be divided as early (A), middle (B) and late (C) stages, based on the depth of membrane edge detected by anti-Myo II antibody staining (Myo II).

To assess whether subcellular trafficking of Notch is affected in *amx*^{mz} embryos, I compared the intracellular distribution of Notch in the ventral-lateral region where the mesoectodermal cells are formed at the early, mid, and late sub-stages of stage 5. I performed double-staining with anti-Notch and anti-Myo II antibodies (Figure 15A-F'), and obtained confocal microscopic images corresponding to the ventral-lateral region of these embryos up to 30µm depth from the apical surface. From these images, I reconstructed Z-section images showing the lateral views of the cells of interest (Figure 15A-F). I defined early, mid, and late sub-stages of stage 5 based on the positions where the tips of lateral membrane (green, white arrowheads) were located (Figure 15A'-F'). At early stage 5, Notch (magenta) is enriched at the apical plasma membrane and apical-lateral membrane in both wild-type (Figure 15A, n=10) and *amx*^{mz} (Figure 15D, n=10) embryos. At mid-stage 5, Notch (magenta) was largely excluded from the apical plasma membrane and detected mostly in the lateral membrane in wild-type embryos in all cases examined (Figure 15B, n=12). However, in *amx*^{mz} embryos at the same stage, Notch (magenta) was still present at the apical plasma membrane and enriched in the apicolateral membrane in 40% of the animals examined (Figure 15E, n=12). At late stage 5, Notch (magenta) was mostly detected in the lateral membrane, as also observed at the mid-stage 5, in wild-type embryos (Figure 15C, n=13). Interestingly in *amx*^{mz} embryos at late stage 5, Notch was also detected in the lateral membrane as observed in the wild-type embryos (Figure 15F, n=17), suggesting that the apical and aplicolateral accumulation of Notch has been relieved between mid and late

stage 5. These results demonstrated that the subcellular distribution of Notch is specifically affected at the mid-stage 5 in *amx*^{mz} embryos, indicating the dynamic nature of this phenotype.

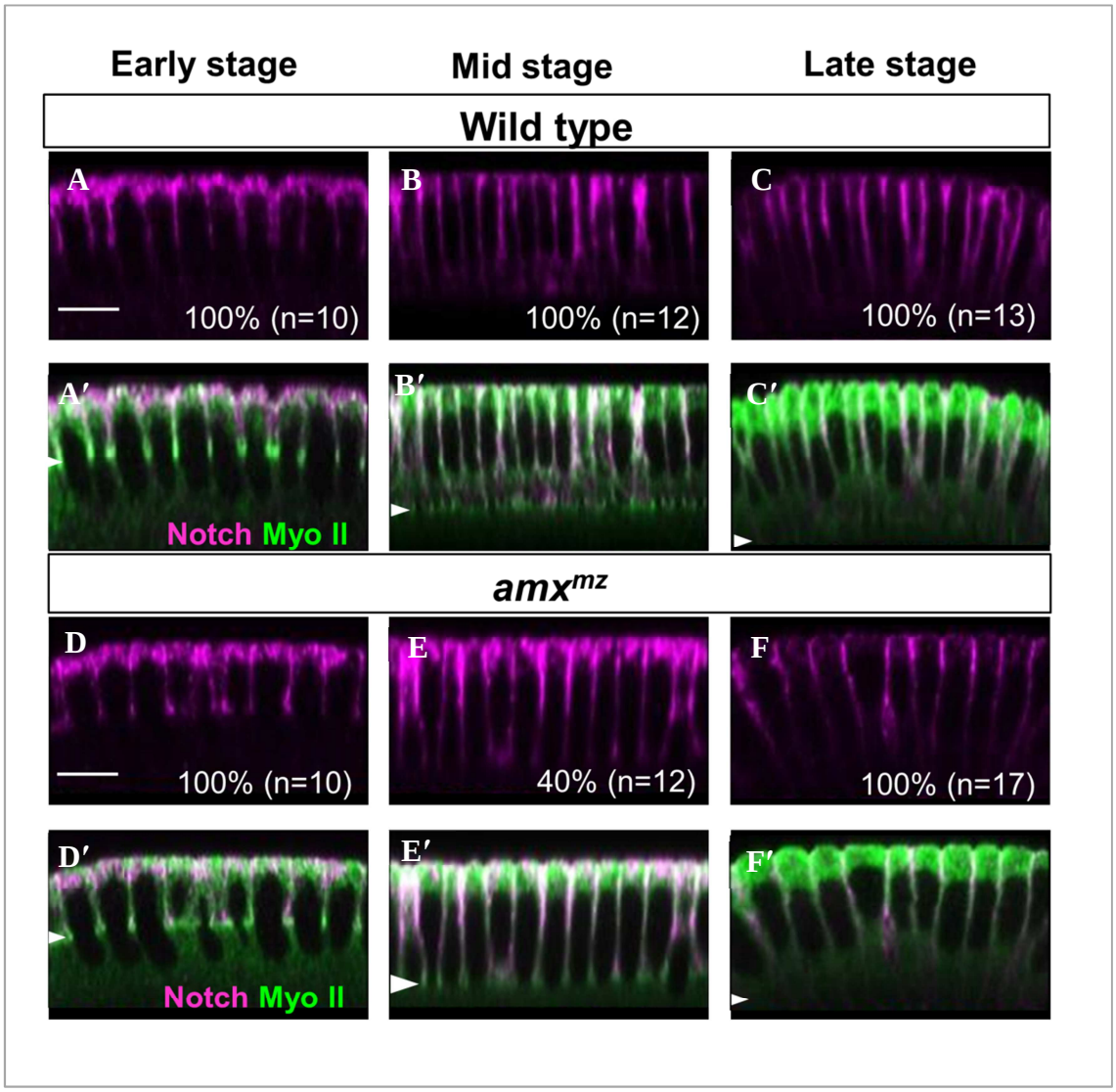

Figure 15: Dynamic Notch distribution is abnormal in *amx*^{mz} embryos at stage 5. The intracellular distribution of Notch (magenta) in wild-type (A-C′) and *amx*^{mz} (D-F′) embryos at the early (A, A′**,** D, D′), middle (B, B′, E, E′), and late (C, C′, F, F′) stage 5, with double-staining of an anti-Myo II antibody (green in A′-F′). Confocal microscopic images corresponding the ventral-lateral region were obtained until 30 µm depth from the apical surface, and Z sections were constructed from them (A-F′). White

arrowheads indicate the position of membrane edges detected by strong anti-Myo II antibody staining (A′-F′). The percentages of embryos showing the presented phenotype are shown in the bottom right. The numbers of embryos examined (n) are shown in parentheses. Scale bar is 10 µm.

To further analyze the abnormal distribution of Notch in *amx*^{mz} embryos at the mid-stage 5, I obtained three higher magnification images every 2 µm from the apical surface of wild-type (from A to A") and *amx*^{mz} embryos (from B to B") (Figure 16A-B").

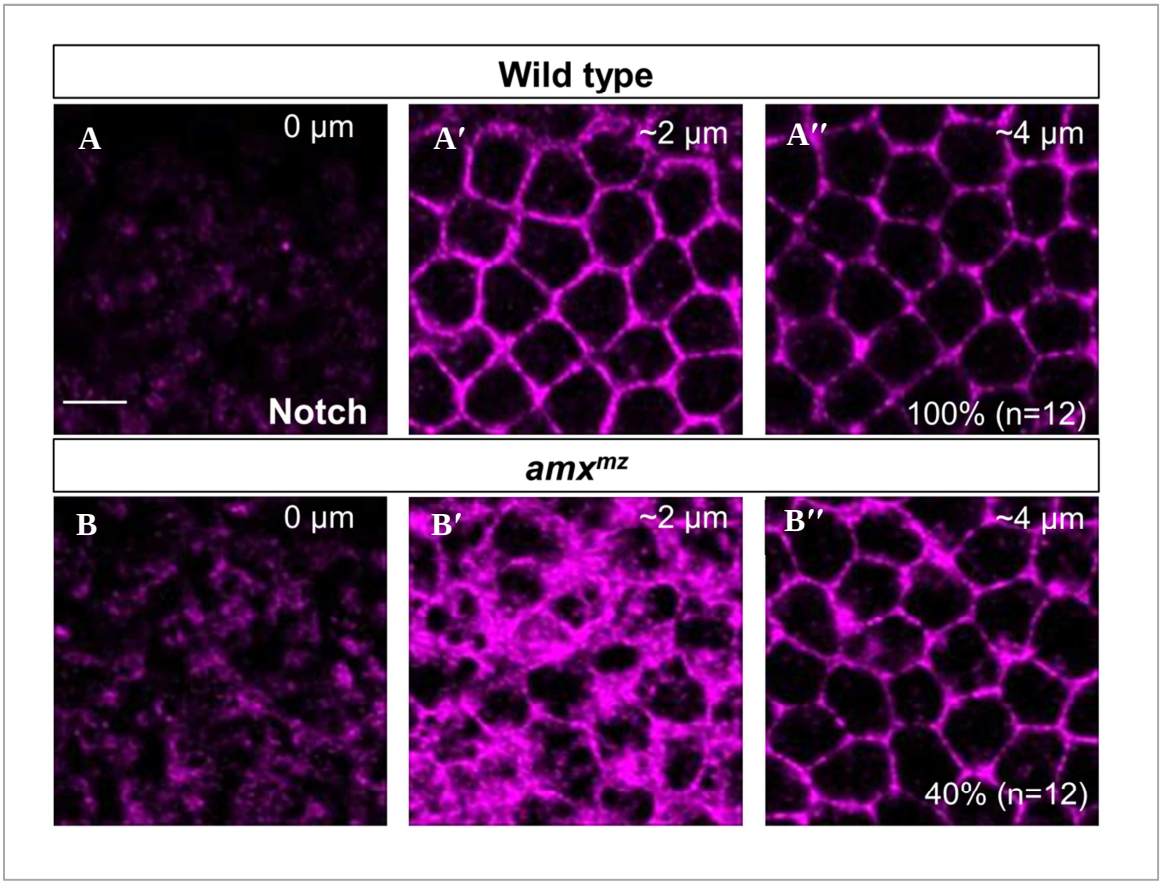

Figure 16: Notch distribution is abnormal in *amx*^{mz} embryos at mid-stage 5. (A-B″) Higher magnification images of X-Y focal planes detecting Notch (magenta) every 2 µm from the apical surface (from A to A″ and from B to B″) of wild-type (A-A″) and *amx*^{mz} (B-B″) embryos at middle stage 5. The percentages of embryos showing the

presented phenotype are shown in the bottom right. The numbers of embryos examined (n) are shown in parentheses. Scale bar is 5 µm.

To objectively evaluate the defective distribution of Notch in the images of wild-type and *amx*^{mz} embryos, I compared the images through a double-blind test. I found that Notch accumulated in a mesh-like structure in *amx*^{mz} embryos in 40% of the embryos examined (Figure17B, n=12), which was never observed in wild-type embryos in all cases examined (Figure 17A, n=12).

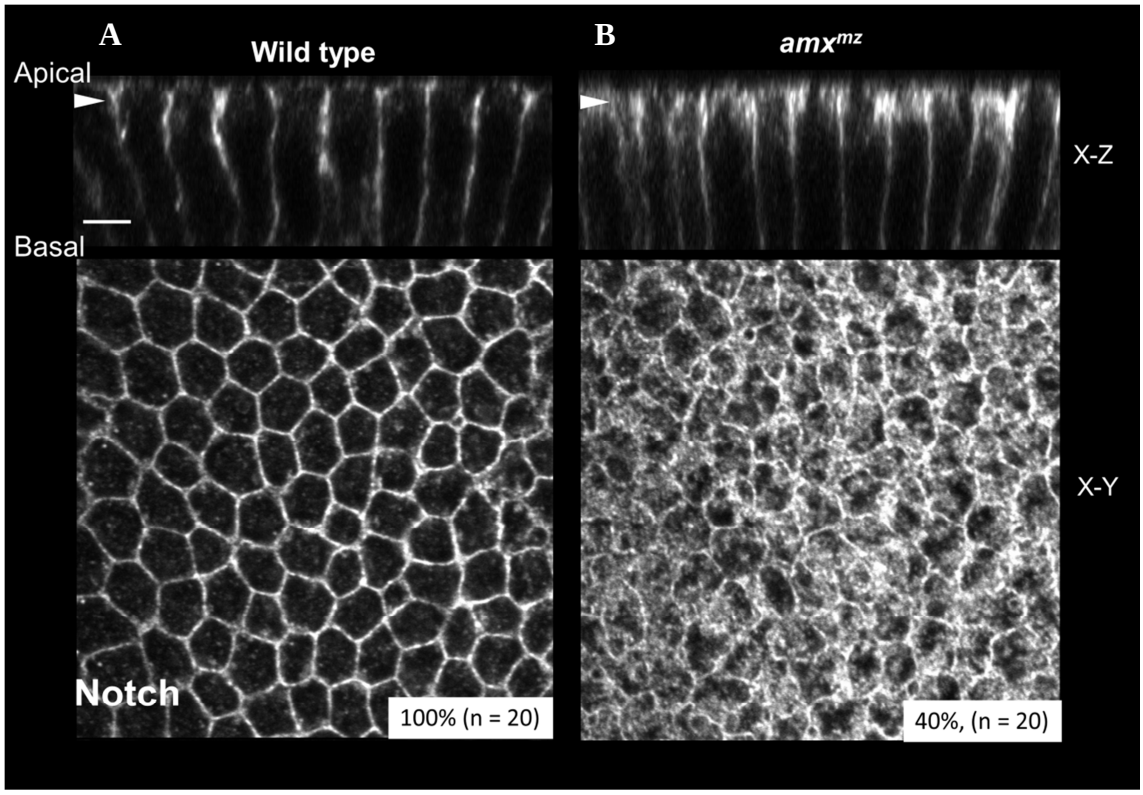

Figure 17: Mesh-like Notch distribution was observed in *amx*^{mz} embryos (A) compared with wild-type (B) at stage 5. The percentages of embryos showing the presented phenotype are shown in the bottom right. The numbers of embryos examined (n) are shown in parentheses. Scale bar is 5 µm.

To confirm this defective distribution of Notch can be specifically attributed to the loss of *amx* function, I examined the distribution of Notch in *amx*^{mz} embryos derived from mothers carrying the *amx[+]* construct (Figure 18A-D''). In these *amx*^{mz} embryos with the *amx* rescue construct, I did not observe the abnormal distribution of Notch at the mid-stage 5 (Figure 18B, n=10), indicating that this defect is due to the maternal loss of *amx*. I obtained the same results by analyzing higher magnification images of X-Y focal planes (Figure 18D-D''). Together, these results suggest that the absence of *amx* function causes the abnormal distribution of Notch in a stage-specific manner in early embryos.

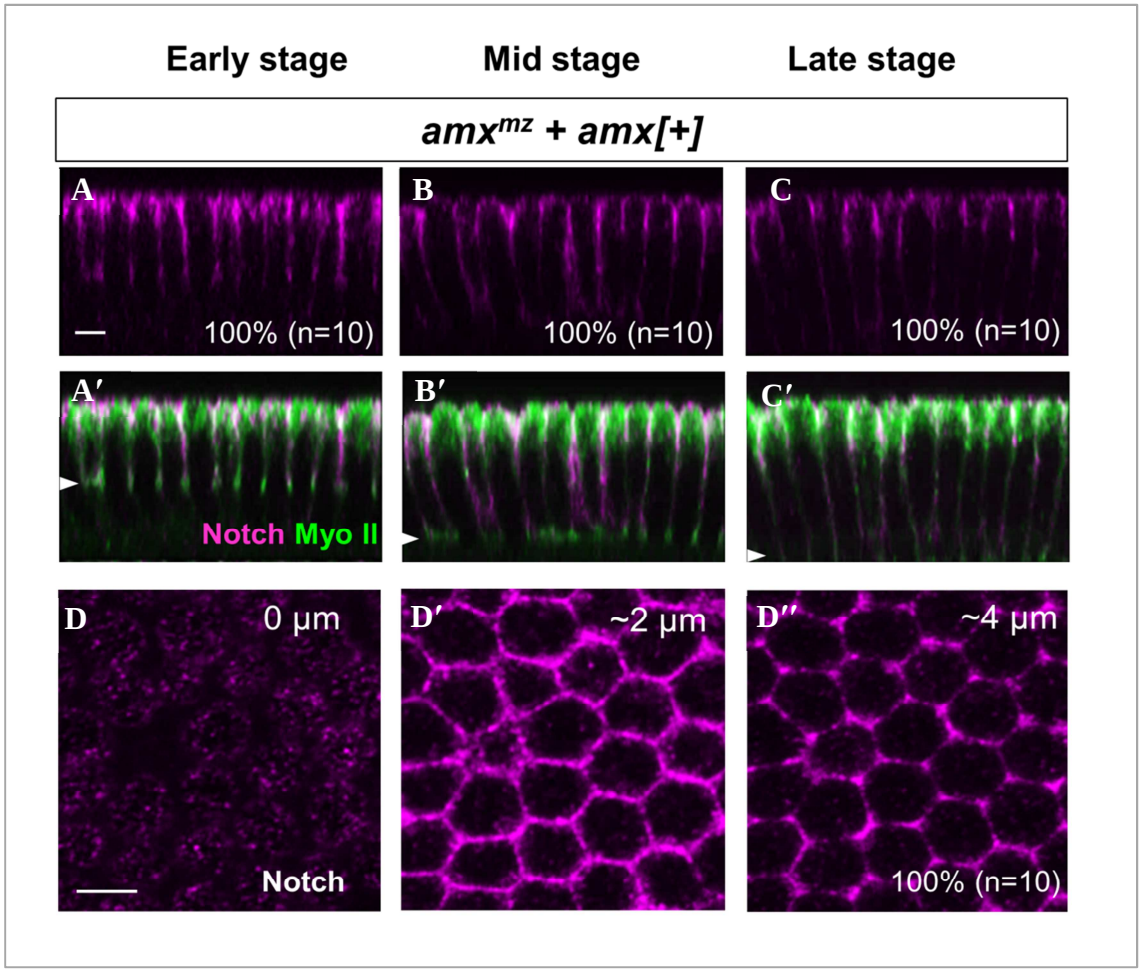

Figure 18: (A-D″) The intracellular distribution of Notch (magenta) in *amx*^{mz} + *amx[+]*embryos at the early (A, A′), middle (B, B′), and late (C, C′) stage 5, with double-staining of an anti-MyoII antibody (green in A′-C′). Confocal microscopic images corresponding the ventral-lateral region were obtained until 30 µm depth from the apical surface, and Z sections were constructed from them (A-C′). White arrowheads indicate the position of membrane edges detected by strong anti-MyoII antibody staining (A′-C′). Higher magnification images of X-Y focal planes detecting Notch (magenta) every 2 µm from the apical surface (from D to D″) of *amx*^{mz} + *amx[+]* embryo at middle stage 5. The percentages of embryos showing the presented phenotype are shown in the bottom right. The numbers of embryos examined (n) are shown in parentheses. Scale bar is 5 µm.

To determine whether the abnormal intracellular distribution of Notch in mid-stage 5 embryo may be a general phenomenon that can be seen in mutants disrupting Notch signaling during mesoectoderm specification, I examined the Notch distribution in the same region of embryos homozygous for *pcx* and lacking its maternal contribution (*pcx*^{mz} embryos) (Figure 19A-D"). Although these embryos are known to show reduced *sim* expression and maternal neurogenic phenotype, similar to *amx*^{mz} embryos (Yamakawa et el., 2012), I did not detect any abnormal intracellular distribution of Notch as observed through Z section (Figure19A-C', n=10 for each) nor in the higher resolution X-Y plane in all cases examined (Figure 19D-D", n=10). This suggests that the transient accumulation of Notch in the apical membrane of the *amx*^{mz} embryos during mid-stage 5 is not a general phenomenon that is associated with defective Notch signaling.

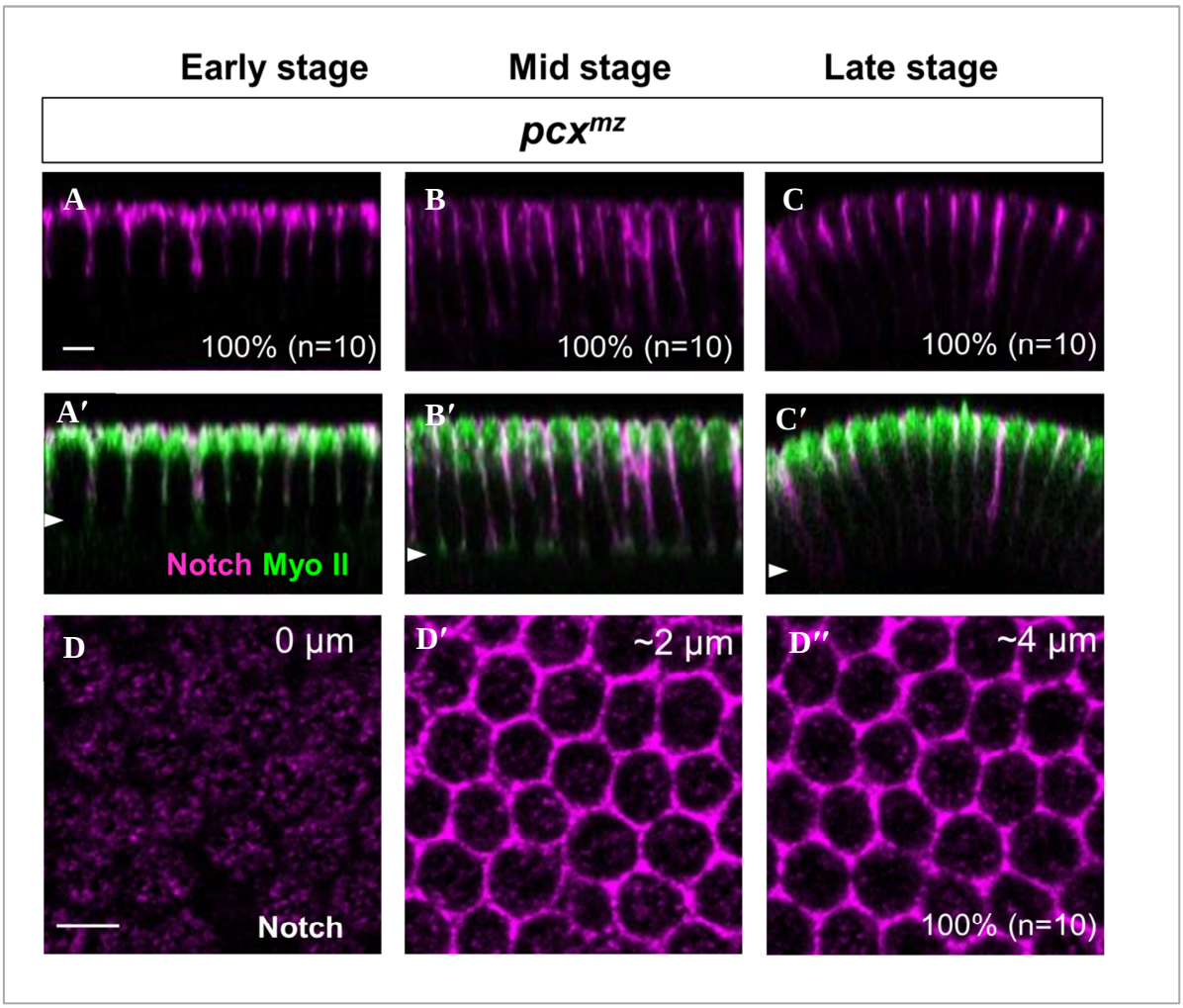

Figure 19: (A-D″) The intracellular distribution of Notch (magenta) in *pcx*^{mz} embryos at the early (A, A′), middle (B, B′), and late (C, C′) stage 5, with double-staining of an anti-MyoII antibody (green in A′-C′). Confocal microscopic images corresponding the ventral-lateral region were obtained until 30 µm depth from the apical surface, and Z sections were constructed from them (A-C′). White arrowheads indicate the position of membrane edges detected by strong anti-MyoII antibody staining (A′-C′). Higher magnification images of X-Y focal planes detecting Notch (magenta) every 2 µm from the apical surface (from D to D″) of *pcx*^{mz} embryo at middle stage 5. The percentages of embryos showing the presented phenotype are shown in the bottom right. The numbers of embryos examined (n) are shown in parentheses. Scale bar is 5 µm.

I next assessed that the observed defects in the subcellular localization of Notch in *amx*^{mz} embryos can also be seen in other membrane bound proteins. I analyzed the subcellular localization of Dl in the ventral-lateral region of wild-type and *amx*^{mz} embryos during stage 5 (Figure 20A-C' and Figure 20E-G'). In Z section images, Dl (magenta) was mostly detected in the apical plasma membrane and apical-lateral membrane at early stage 5 in wild-type embryos, which was reminiscent of Notch distribution at the same stage (Figure 20A). At mid and late stage 5, Dl was detected in the lateral membrane and diminished from apical plasma membrane in wild-type embryos, similar to the temporal change of Notch distribution in wild-type embryos (Figure 20B,C). However, in contrast to the abnormal distribution of Notch in *amx*^{mz} embryos, the subcellular distribution of Dl did not show marked difference between *amx*^{mz} (n=46) and wild-type embryos (n=31) at all three periods of stage 5 (Figure 20E-G). In the higher resolution X-Y focal planes, I also observed that Dl distribution is not affected in *amx*^{mz} embryos at mid-stage 5 (Figure 20H-H") compared with wild-type (Figure 20D-D"). These results suggested that the defect of Notch distribution at mid-stage 5 is not due to a general subcellular trafficking defect.

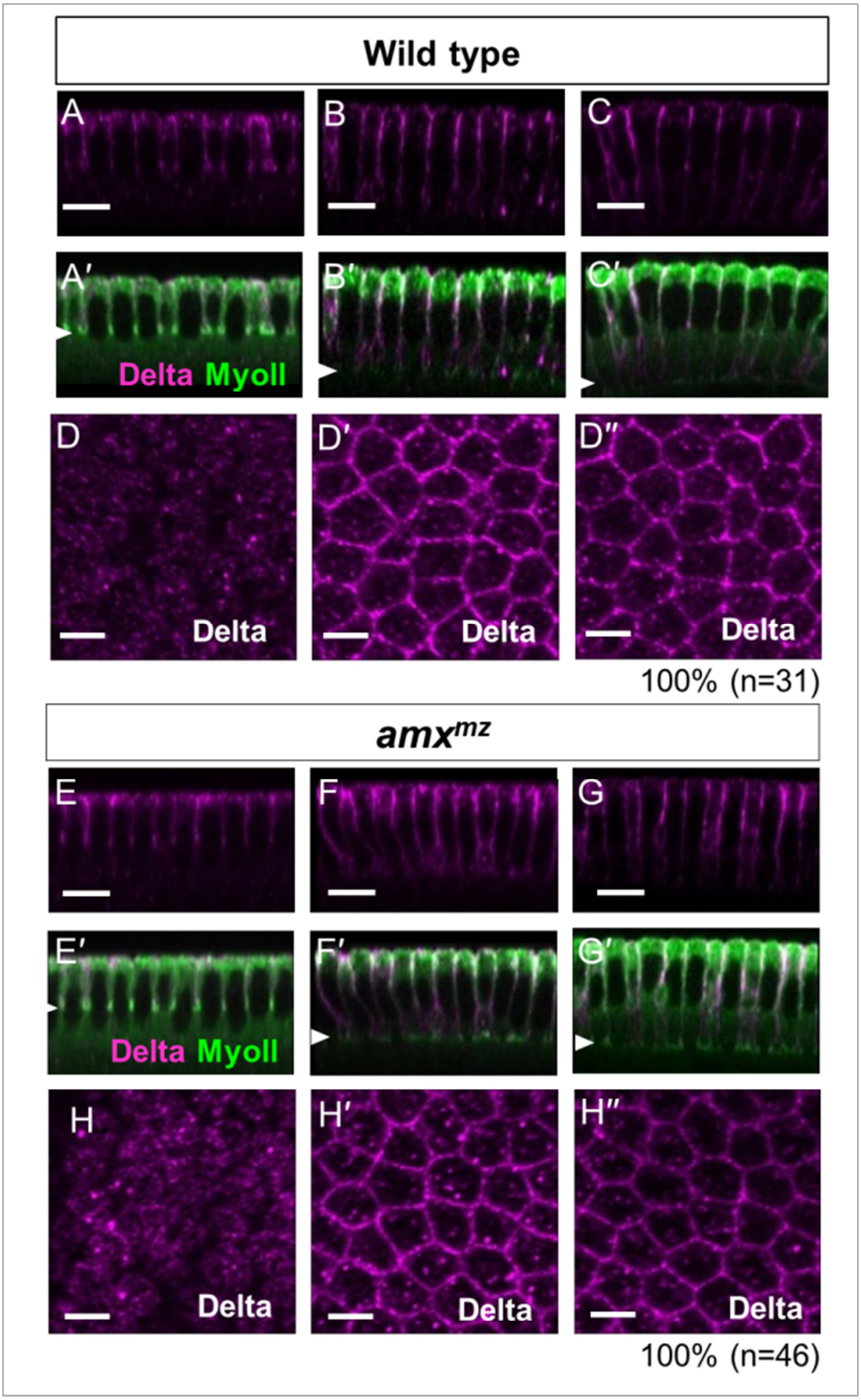
Wild type
A
B
C
A′
B′
C′
Delta MyoII
D
D′
D″
Delta
100% (n=31)
amx^mz
E
F
G
E′
F′
G′
Delta MyoII
H
H′
H″
Delta
100% (n=46)

Figure 20: The subcellular localization of Delta is normal in *amx*^{mz} embryos at stage 5. (A-C′ and E-G′) The intracellular distribution of Delta (magenta) in wild-type (A-C′) and *amx*^{mz} (E-G′) embryos at the early (A, A′, E, and E′), middle (B, B′, F, and F′), and late (C, C′, G, and G′) stage 5, with double-staining of an anti-MyoII antibody (green in A′-C′ and E′-G′). Confocal microscopic images corresponding the ventral-lateral region were obtained until 30μm depth from the apical surface, and Z sections were constructed from them (A-C′ and E-G′). White arrowheads indicate the position of membrane edges detected by strong anti-MyoII antibody staining (A′-C′ and E′-G′). (D-D″ and H-H″) Higher magnification images of X-Y focal planes detecting Delta (magenta) every 2 μm from the apical surface (from D to D″ and from H to H″) of wild-type (D-D″) and *amx*^{mz} (H-H″) embryos at middle stage 5. The percentages of embryos showing the presented phenotype are shown in the bottom right. The numbers of embryos examined (n) are shown in parentheses. Scale bar is 5 μm.

3.4 The structure of the apical membrane is not altered in amx^{mz} embryos

I detected the abnormal distribution of Notch in the apical and apical-lateral membrane at mid-stage 5 in *amx*^{mz} embryos, which coincides with the period when the apical structure of cells changes drastically (Figure 15-17). Since microvilli that are observed at early stage 5 decreases and eventually disappears during the mid and late stage 5, I assessed whether there are any gross structural changes in the apical and apical-lateral membrane in *amx*^{mz} embryos. To analyze the structure of these membranous regions, I visualized the plasma membrane using anti-Sec5 antibody staining (Murthy et al., 2003).

I did not detect marked difference in the pattern of Sec5 staining between wild-type (n=5) and *amx*^{mz} (n=5) embryos at early and mid-stage 5, suggesting that there is no structural alterations either in the apical or in the apical-lateral membranes (Figure

21A-D). Next, I imaged F-Actin that is enriched in the microvilli to further assess whether there may be a structural change in the cytoskeletal structure underneath the apical and apical lateral membrane. Similar to anti-Sec5 immunostaining, I did not detect any differences in the F-Actin signal between wild-type (n=7) and *amx*^{mz} (n=7) embryos at early and mid-stage 5 (Figure 21E-H). Taken these results together, I did not detect a major change in the structures of the plasma membrane and cytoskeleton. Therefore, the altered subcellular localization of Notch in *amx*^{mz} embryos cannot be attributed to the structure of plasma membrane and cytoskeleton, although I cannot rule out a possibility that there may be subtle and undetectable changes in these structures.

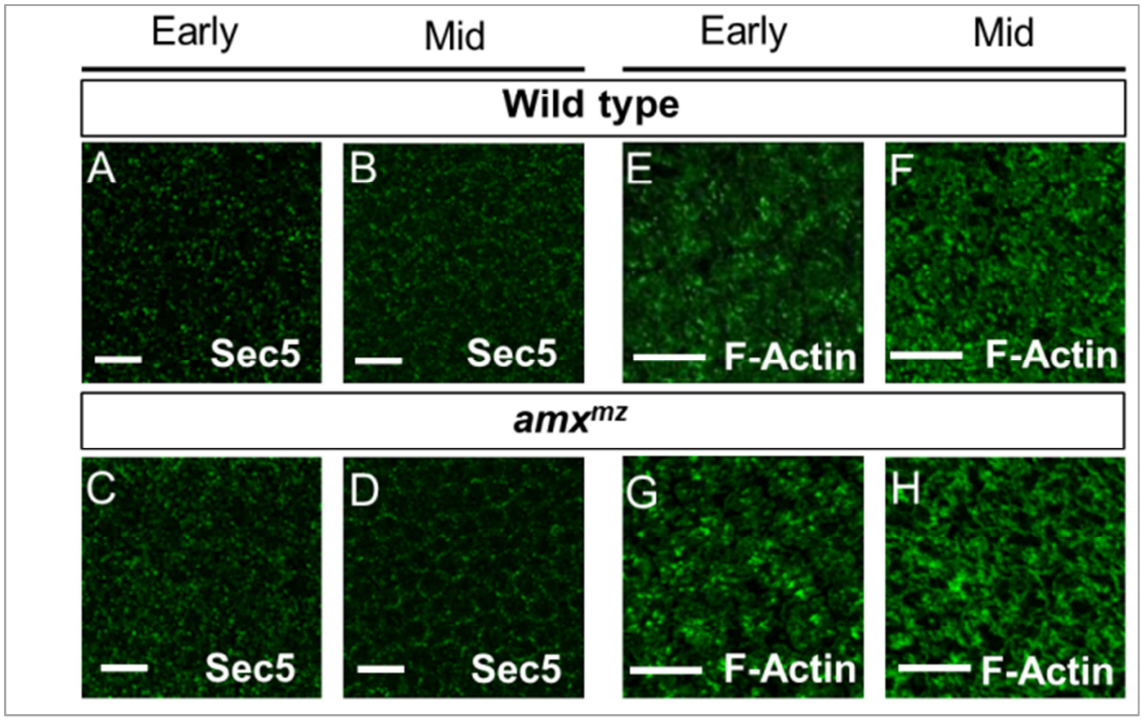

Figure 21: The structure of the apical membrane did not show abnormalities in *amx*^{mz} embryos. (A-D) The intracellular distribution of Sec5 (green) in wild-type (A, B) and *amx*^{mz} (C, D) embryos at early (A, C) and middle (B, D) stage 5. X-Y images of focal

planes representing 2 µm below from the apical surface are shown. (E-H) The distribution of F-actin (green) detected by phalloidin staining in wild-type (E, F) and *amx*^{mz} (G, H) embryos at early (E, G) and middle (F, H) stage 5. X-Y images of focal planes representing 2 µm below from the apical surface are shown. The percentages of embryos showing the presented phenotype are shown in the bottom right. The numbers of embryos examined (n) are shown in parentheses. Scale bar is 10 µm.

3.5 Notch accumulates in a subcellular compartment that does not coincide with major exocytic or endocytic markers in amx^{mz} embryos

In order to understand the nature of Notch mislocalization in the absence of *amx*, I attempted to determine the intracellular compartment(s) where Notch abnormally accumulates in *amx*^{mz} embryos at mid-stage 5 though co-immunostaining and confocal imaging (Figure 22 and Figure 23).

First, I analyzed the potential colocalization of Notch with markers of endoplasmic reticulum (ER) (Pdi-GFP) and Golgi apparatus (*cis*-Golgi matrix protein, GM130; *trans*-Golgi marker, PNA-Lectin) (Yano et al., 2005; O'Sullivan et al., 2012). I found that Notch does not markedly colocalize with the ER or Golgi markers in both wild-type and *amx*^{mz} embryos in all cases examined (Figure 22A-F, n=10 for each). In addition, the overall staining pattern of ER and Golgi did not show detectable abnormality in *amx*^{mz} embryos, compared with those of wild type (Figure 22A-F).

I next examined whether Notch abnormally accumulates in endocytic compartments, including recycling (Rab11) (Tanaka & Nakamura, 2008), early (Hrs) (Lloyd et al., 2002), and late (Rab7) (Tanaka & Nakamura, 2008) endosomes in *amx*^{mz} embryos. However, I did not observe significant colocalization between Notch and

these markers in *amx*^{mz} embryos compared with those of wild-type embryos in call cases examined (Figure 23G-L, n=10 for each). I also found that the overall morphology and numbers of these endocytic compartments appeared normal in *amx*^{mz} embryos, as compared with those of wild type (Figure 23G-L). Therefore, at this point, I were unable to determine the identity of the mesh-like subcellular structure(s) where Notch abnormally accumulates in *amx*^{mz} embryos.

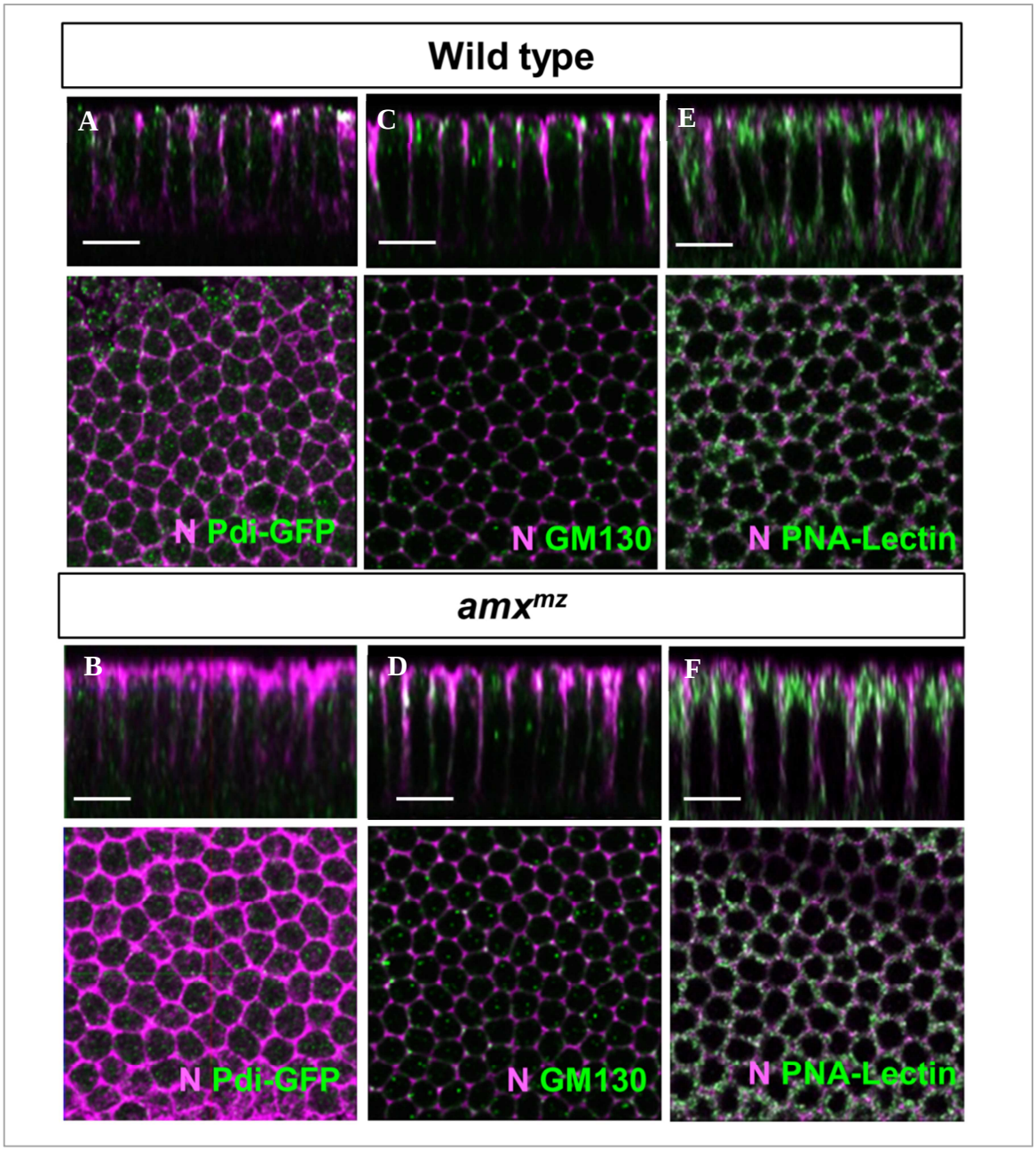

Figure 22: Abnormally accumulated Notch was not detected in typical exocytic compartments in *amx*^{mz} embryos. (A-F) The colocalization of Notch (magenta) with the various markers of exocytic compartments (green), including ER (Pdi-GFP) (A, B) and *cis*-Golgi apparatus (GM130) (C, D), *trans*-Golgi (PNA-Lectin) (E, F) in wild-type (A, C, and E) and *amx*^{mz} (B, D, and F) embryos. The upper panels represent Z sections constructed from the images obtained until 30 µm depth from the apical surface. The lower images represent X-Y images of focal planes representing 2 µm below from the apical surface. 10 embryos were analyzed in each experiment and all showed the same results represented by each picture. Scale bar 10 µm.

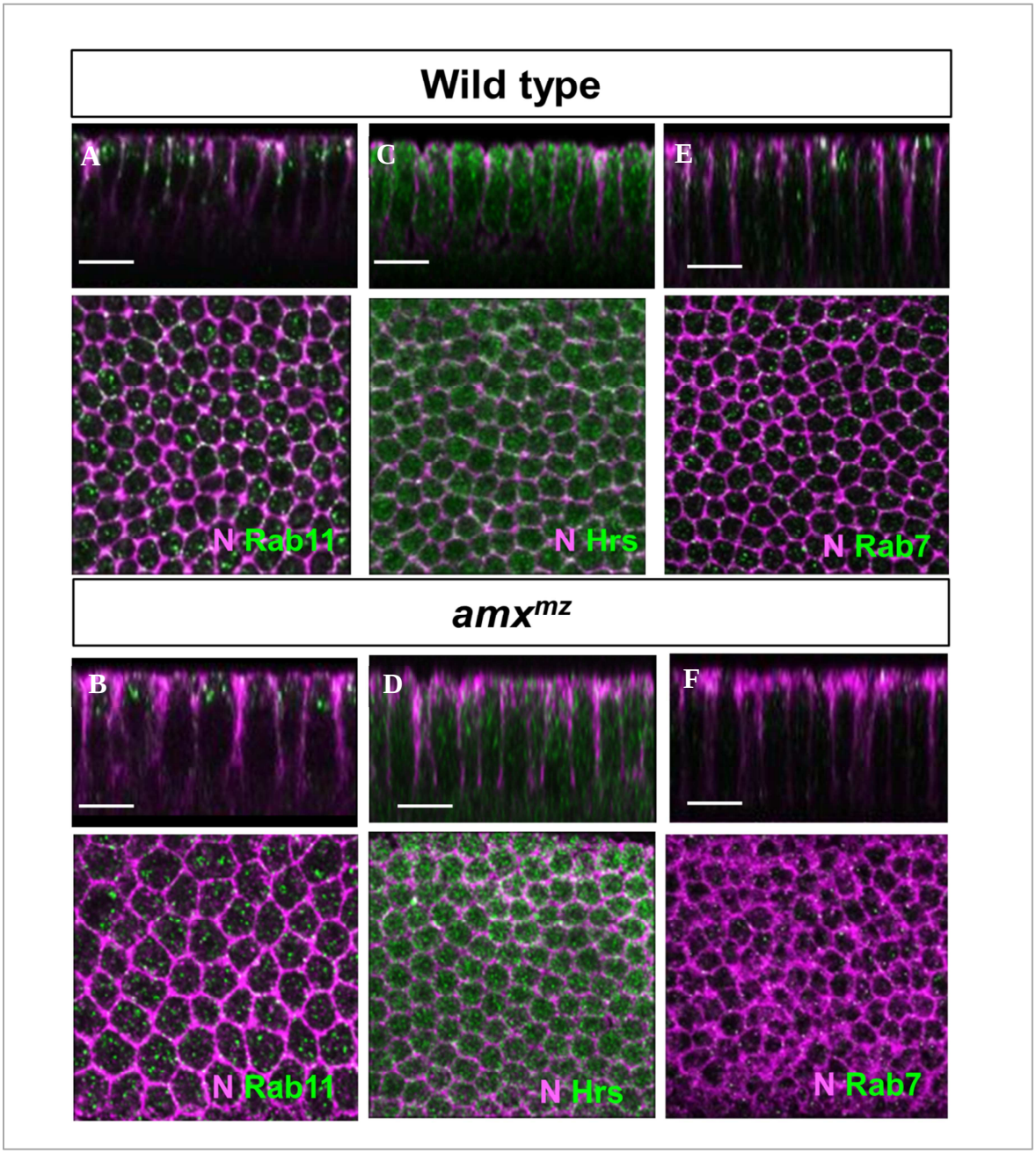

Figure 23: Abnormally accumulated Notch was not detected in typical endocytic compartments in *amx*^{mz} embryos. (A-F) The colocalization of Notch (magenta) with the various markers of endocytic compartments (green), including recycling endosomes (Rab11) (A,B), early endosomes (Hrs) (C,D), and late endosomes (Rab7) (E,F) in wild-type (A, C, and E) and *amx*^{mz} (B, D, and F) embryos. The upper panels represent Z sections constructed from the images obtained until 30 µm depth from the apical surface. The lower images represent X-Y images of focal planes representing 2 µm below from the apical surface. 10 embryos were analyzed in each experiment and all showed the same results represented by each picture. Scale bar 10 µm.

4. Discussion

4.1 Requirements of amx for Notch signaling is context-dependent

Consistent with *amx*^{1} and *amx*^{m} alleles reported previously, my analysis of the first clean null allele of *amx*, (*amx*^{N}), showed that this gene is clearly required maternally to facilitate Notch signaling during early embryogenesis. In contrast to a previous study demonstrating that *amx* is also required zygotically for the imaginal development using the *amx*^{m} allele (Michellod et al., 2003), I found that, there are no observable morphological phenotypes in *amx*^{N} zygotic mutant flies, as previously found in *amx*^{1} zygotic mutant. Considering that *amx*^{m} is a complex allele that potentially affects genes other than *amx*, I conclude that the observed zygotic phenotypes of the *amx*^{m} allele are due to defects in other genes.

By assessing the phenotypes of *amx*^{mz} embryos, I identified that *amx* not only is required for neuroectoderm specification during mid-embryogenesis but also required for mesoectoderm specification during early embryogenesis (Figure 11 and Figure 13). It is known that the *sim* expression in the mesoectodermal cells depends on Notch signaling, because in various mutants in core Notch signaling pathway genes, including

Notch and *Suppressor of Hairless*, the expression of *sim* becomes restricted to very few cells (Lecourtois & Schweisguth, 1995; Morel & Schweisguth, 2000). Interestingly, expression of *sim* was only reduced partially in amx^{mz} embryos, although these embryos demonstrated strong neurogenic phenotype with full penetration. These results revealed that *amx* is partially required for the activation of Notch signaling in the mesoectodermal cells, which is reminiscent of *pecanex* (*pcx*) gene (Yamakawa et al., 2012). *pcx* is also a maternal neurogenic gene and exhibits a strong neuroblast segregation defect while being partially required for the activation of *sim* during mesoectodeerm specification (Yamakawa et al., 2012). One interpretation of this differential contribution is that *amx* and *pcx* are absolutely required in neuroectodermal cells whereas they are only partially required for mesoectoderm specification. Considering that neuroectoderm segregation is mediated by "lateral inhibition" through Notch signaling, whereas mesoectoderm specification happens through "inductive signaling", the two events may be regulated differently by *amx, pcx* and other genes. Alternatively, *amx* and *pcx* may be involved in facilitating Notch signaling in both contexts, but the neuroblast selection process requires a higher level of Notch activation than mesoectoderm specification. This issue could be clarified by assessing whether Notch activity is partially or completely abolished during the two developmental processes in *amx* and *pcx* mutants using more sensitive assays *in vivo*.

4.2 Amx may regulate the intracellular distribution of Notch in a specific time window during early embryogenesis

Our analysis here demonstrated that the subcellular distribution of the Notch receptor, but not the Dl ligand, depends on a function of maternal *amx* in the early

cellularization stage (mid-stage 5) (Figure 15, Figure 16, Figure 17, Figure 20 and Figure 24). During this stage, the structure of apical plasma membrane with microvilli changes drastically (Figard et al., 2013, 2016). Through immunostaining studies, I found that the structures of the apical plasma membrane and the F-Actin were not detectably altered in the absence of *amx* function (Figure 21). Together with the observations that ER, Golgi, and endosome morphology seems to be unaltered, *amx* has specific role in regulating Notch trafficking during this stage (Figure 22, Figure 23 and Figure 24).

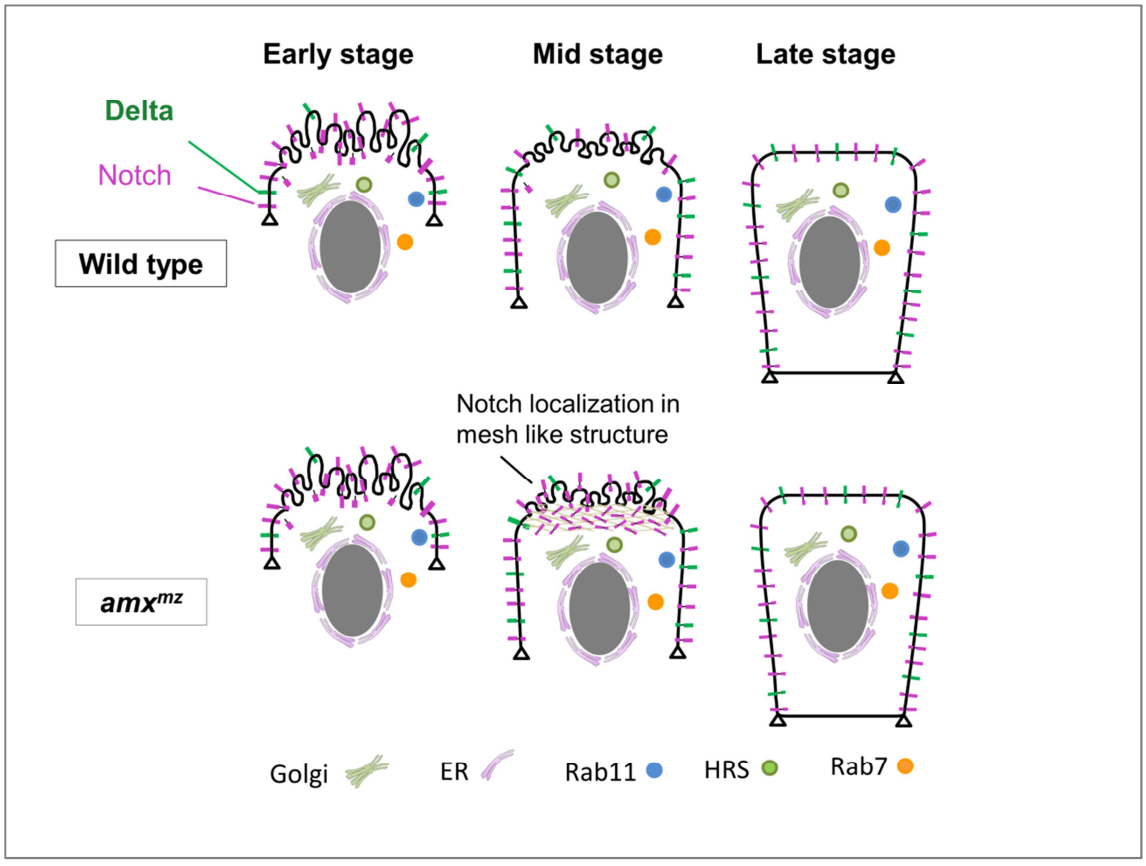

Figure 24: Illustration showing abnormal, subcellular, mesh-like Notch distribution in *amx*^{mz} embryos at mid-stage 5, which neither changed nor co-localized with ER, Golgi and any endocytic compartments.

In *amx*^{mz} embryos at mid-stage 5, I observed that Notch is abnormally accumulated in a mesh-like subcellular structure (Figure 16 and Figure 17). Although I examined the potential colocalization of Notch with markers for the ER, Golgi apparatus, and various endosomal compartments, I failed to determine where Notch is abnormally accumulated (Figure 22 and Figure 23). Therefore, at this point, it remains unknown in which intracellular compartment(s) Notch is mislocalized in the absence of *amx* functions. It is important to note, however, that the mislocalization of Notch in *amx*^{mz} embryos is not a consequence of the aberrant Notch signaling, because Notch localization in *pcx*^{mz} embryos was not changed in mid-stage 5 embryos (Figure 19). Although I cannot conclude whether the mislocalization of Notch is a cause of the reduction or depletion of Notch signaling in the absence of *amx* functions, it is tempting to speculate that this trafficking defect of Notch is contributing to defective Notch signaling. Vesicular trafficking of Notch can facilitate either activation or inhibition of the signaling depending on the context (Yamamoto et al., 2010; Baron, 2012). Importantly, endocytic trafficking of Notch was found to facilitate S3 cleavage of Notch, likely because γ-secretase cleavage is a pH dependent protease that is more active at acidic environments such as in the late endosome (Gupta-Rossi et al., 2004; Vaccari, 2008). Considering that previous epistasis analysis involving *amx* and full-length and activated forms of Notch placed Amx in the S3 cleavage step of signal transduction (Michellod & Randsholt, 2008), it would be interesting to further explore the relationship between this trafficking defect of Notch and γ-secreatse-mediated S3 cleavage. To understand the precise roles of Amx in the activation of Notch additional experiments, such as live-imaging analyses of Notch intracellular trafficking would be informative (Couturier, 2014; Trylinski, 2017).

4.3 Amx family proteins and their links to Alzheimer's disease

While *amx* and its related genes are evolutionarily conserved between *Drosophila* and vertebrate species including human, the function of this protein family is still obscure (Kajkowski et al., 2001; Michellod & Randsholt, 2008). The *amx* family genes (*CG10795, CG11103* and *amx* in *Drosophila*, *TM2D1-3* in human) encode predicted double-pass transmembrane proteins with a conserved DRF motif (Michellod & Randsholt, 2008). DRF motifs found in some G-protein coupled receptors have been shown to mediate conformational changes upon ligand binding (Koenen et al., 2017), but the function of this motif within Amx family proteins have yet to be defined (Lee et al., 2003). Recently, a rare missense (p.P155L) variant affecting the CTLD of *TM2D3*, the human ortholog of *amx*, was identified as a risk allele for late-onset Alzheimer's disease in an Icelandic population (Jakobsdottir et al., 2016). One pathological hallmark of Alzheimer's disease is deposition of plaques of β-amyloid, which is produced γ-secretase mediated cleavage of β-amyloid precursor protein (APP). Together with the genetic evidence, it is more likely that amx participates in Notch signaling at the S3 cleavage step of Notch activation (Michellod & Randsholt, 2008). Jakobsdottir et al. (2016) proposed that Amx/TM2D3 may contribute directly or indirectly to the γ-secretase cleavage of Notch and APP, a hypothesis that needs to be tested biochemically. More recently, *TM2D1-3* were identified as regulators of phagocytosis based on a CRISPR based screens using human phagocytic cell lines (Haney et al., 2018). Considering that *TM2D1* have been found to physically interact with Aβ42 (Kajkowski et al., 2001) and cellular knockout of *TM2D1*, *TM2D2* or *TM2D3* can diminish the ability of cells to phagocytose Aβ peptides in vitro, Haney et al. (2018) proposed that these proteins may be involved in Alzhemier's disease through regulation of amyloid

clearance in the brain. It is important to note that these hypotheses are not mutually exclusive, and defects in cellular events such as intracellular trafficking may lead to defects in both γ-secretase mediated APP processing as well as phagocytic clearance of Aβ42.

5. References

Arora P. S., Ansari A. Z. (2009). Chemical biology: A Notch above other inhibitors. *Nature. 462 (7270),* 171-173. doi:10.1038/462171a.

Artavanis-Tsakonas, S. (1996). The intracellular deletions of Delta and Serrate define dominant negative forms of the *Drosophila* Notch ligands. *Development, 122(8),* 2465-74.

Artavanis-Tsakonas, S., Matsuno, K., & Fortini, M. E. (1995). Notch Signaling. *Science, 268 (5208),* 225-232.

Artavanis-Tsakonas, S., Rand, M. D., & Lake, R. J. (1999). Notch signaling: cell fate control and signal integration in development. *Science, 284,* 770-776. doi: 10.1126/science.284.5415.770.

Austin J., & Kimble J. (1987). glp-1 is required in the germ line for regulation of the decision between mitosis and meiosis in *C. elegans*. *Cell, 51(4),* 589–599. doi:10.1016/0092-8674(87)90128-0.

Austin J., & Kimble J. (1989). Transcript analysis of *glp-1* and *lin-12*, homologous genes required for cell interactions during development of *C. elegans*. *Cell, 58(3),* 565–71. doi:10.1016/0092-8674(89)90437-6.

Baron, M. (2012). Endocytic routes to Notch activation. *Seminars in Cell & Developmental Biology, 23(4),* 437-42. doi: 10.1016/j.semcdb.2012.01.008.

Bhandari D. R., Seo K. W., Roh K. H., Jung J. W., & Kang K. S. (2010). REX-1 expression and p38 MAPK activation status can determine proliferation/differentiation fates in human mesenchymal stem cells. *PLoS One*. 5 (5), e10493. doi:10.1371/journal.pone.0010493.

Bopp, D., Bell, L. R., Cline, T. W., & Schedl, P. (1991). Developmental distribution of female-specific Sex-lethal proteins in *Drosophila melanogaster*. *Genes & Development, 5,* 403-415.

Bray, S. J. (2006). Notch signaling: a simple pathway becomes complex. *Nature Reviews Molecular Cell Biology, 7,* 678–689. doi:10.1038/nrm2009.

Cooper, H. M., & Paterson, Y. (1995). Induction of immune responses. *Current Protocols in Immunology,2.4.1-2.4.9.*

Couturier, L., Trylinski, M., Mazouni, K., Darnet, L., & Schweisguth, F. (2014). A fluorescent tagging approach in *Drosophila* reveals late endosomal trafficking of Notch and Sanpodo. *Journal of Cell Biology, 207(3),*351-63. doi: 10.1083/jcb.201407071.

de Celis J. F., & Bray S. J. (2000). The Abruptex domain of Notch regulates negative interactions between Notch, its ligands and Fringe. *Development*. *127 (6),* 1291-1302.

de la Concha, A., Dietrich, U., Weigel, D., & Campos-Ortega, J. A. (1988). Functional interactions of neurogenic genes of *Drosophila melanogaster. Genetics, 118*, 499-508

Fehon, R. G., Kooh, P. J., Rebay, I., Regan, C. L., Xu, T., Muskavitch, M. A., & Artavanis-Tsakonas, S. (1990). Molecular interactions between the protein products of the neurogenic loci Notch and Delta, two EGF-homologous genes in *Drosophila*. *Cell, 61,* 523-534.

Figard, L., Wang, M., Zheng, L., Golding, I., & Sokac, A. M. (2016). Membrane supply and demand regulates F-Actin in a cell surface reservoir. *Developmental Cell, 37,* 267-278.

Figard, L., Xu, H., Hernan, G., Golding, I., & Sokac A. M. (2013). The Plasma membrane flattens out to fuel cell-surface growth during *Drosophila* cellularization. *Developmental Cell, 27,* 648-655.

Fryer, C. J., White, J. B., & Jones, K. A. (2004). Mastermind recruits CycC:CDK8 to phosphorylate the Notch ICD and coordinate activation with turnover. *Molecular Cell, 16,* 509-520.

Gordon, W. R., Arnett, K. L., & Blacklow, S. C. (2008). The molecular logic of Notch signaling – a structural and biochemical perspective. *Journal of Cell Science, 121,* 3109-3119. doi:10.1242/jcs.035683.

Greenwald I. (1985). lin-12, a nematode homeotic gene, is homologous to a set of mammalian proteins that includes epidermal growth factor. *Cell, 43,* 583-590. doi:10.1016/0092-8674(85)90230-2.

Greenwald I. S., Sternberg P. W., & Horvitz H. R. (1983). The lin-12 locus specifies cell fates in *Caenorhabditis elegans*. *Cell, 34(2),* 435–444. doi: 10.1016/0092-8674(83)90377-x.

Gupta-Rossi, N., Six, E., LeBail, O., Logeat, F., Chastagner, P., Olry, A., … & Brou, C. (2004). Monoubiquitination and endocytosis direct γ-secretase cleavage of activated Notch receptor. *The Journal of Cell Biology, 166,* 73-83.

Guruharsha, K. G., Kankel, M. W., & Artavanis-Tsakonas, S. (2012). The Notch signaling system: recent insights into the complexity of a conserved pathway. *Nature Review Genetics, 13(9),* 654–666.

Haney, M. S., Bohlen, C. J., Morgens, D. W., Ousey, J. A., Barkal, A. A., Tsui, C. K., … & Bassik, M. C. (2018). Identification of phagocytosis regulators using

magnetic genome-wide CRISPR screens. *Natute Genetics, 50(12),* 1716-1727. doi: 10.1038/s41588-018-0254-1.

He, B., Martin, A., & Wieschaus, E. (2016). Flow-dependent myosin recruitment during *Drosophila* cellularization requires zygotic dunk activity. *Development, 143,* 2417-2430. doi:10.1242/dev.131334.

Jakobsdottir, J., van der Lee, S. J., Bis, J. C., Chouraki, V., Li-Kroeger, D., Yamamoto, S., & Aspelund, T. (2016). Rare functional variant in TM2D3 is associated with Late-Onset Alzheimer's Disease. *PLoS Genetics, 12*, e1006327. doi: 10.1371/journal.pgen.1006327.

Johansen, M. K., Fehon, G. R., & Artavanis-Tsakonas, S. (1989). The *Notch* gene product is a glycoprotein expressed on the cell surface of both epidermal and neuronal precursor cells during *Drosophila* development. *The Journal of Cell Biology, 109,* 2427-2440.

Kajkowski, E. M., Lo, C. F., Ning, X., Walker, S., Sofia, H. J., Wang, W., & Ozenberger, B. A. (2001). beta -Amyloid peptide-induced apoptosis regulated by a novel protein containing a g protein activation module. *The Journal of Biological Chemistry, 276(22),* 18748-56.

Kelley, L. A., Mezulis, S., Yates, C. M., Wass., M. N. & Sternberg, M. J. (2015). The Phyre2 web portal for protein modeling, prediction and analysis. *Nature Protocols, 10(6),* 845-58.

Kelso, R. J., Buszczak, M. , QuinÄones, A. T ,Castiblanco, C., Mazzalupo, S., & Cooley, L. (2004). Flytrap, a database documenting a GFP protein-trap insertion screen in *Drosophila melanogaster*. *Nucleic Acids Research, 32*, D418-D420.

Kidd, S., Baylies, M. K., Gasic, G. P., & Young, M. W. (1989). Structure and distribution of the Notch protein in developing *Drosophila*. *Genes & Development, 3,* 1113-I 129.

Koenen A., Babendreyer A., Schumacher J., Pasqualon T., Schwarz N., Seifert A., Deupi X., Ludwig A., & Dreymueller D. (2017) The DRF motif of CXCR6 as chemokine receptor adaptation to adhesion. *PLoS ONE*, *12(3),* e0173486. doi: 10.1371/journal.pone.0173486.

Kopan, R., & Ilagan, M. X. (2009). The canonical Notch signaling pathway: unfolding the activation mechanism. *Cell, 137,* 216-33. doi: 10.1016/j.cell.2009.03.045.

Kovall, R. A., & Blacklow, S. C. (2010). Mechanistic insights into Notch receptor signaling from structural and biochemical studies. *Current Topics in Developmental Biology, 92,* 31-71.

Kovall, R. A., Gebelein, B., Sprinzak, D., & Kopan, R. (2017). The canonical Notch signaling pathway: structural and biochemical insights into shape, sugar, and force. *Developmental Cell, 41(3),* 228-241.

LaBonne, S. G., & Mahowald, A. P. (1985). Partial rescue of embryos from two maternal-effect neurogenic mutants by transplantation of wild-type ooplasm. *Development Biology, 110,* 264-267.

Lecourtois, M., & Schweisguth, F. (1995). The neurogenic Suppressor of Hairless DNA-binding protein mediates the transcriptional activation of the *Enhancer of split complex* genes triggered by Notch signaling. *Genes & Development, 9,* 2598-2608.

Lee Y., Chang D. J., Lee Y. S., Chang K. A., Kim H., Yoon J. S., Lee S., Suh Y. H., & Kaang B. K. (2003). Beta-amyloid peptide binding protein does not couple to G

protein in a heterologous Xenopus expression system. *Journal of Neuroscience Research., 73(2),* 255-159. doi: 10.1002/jnr.10652.

Lehmann, R., Dietrich, U., Jimenez, F., & Campos-Ortega, J. A. (1981). Mutations of early neurogenesis in *Drosophila*. *Wilhelm Roux's Archives, 190,* 226-229.

Lehmann, R., Jimenez, F., Dietrich, U., & Campos-Ortega J. A. (1983). On the phenotype and development of mutants of early neurogenesis in *Drosophila melanogaster*. *Roux's Archive of Development Biology, 192,* 62-74.

Li-Kroeger, D., Kanca, O., Lee, P. T., Cowan, S., Lee, M. T., Jaiswal, M., …Bellen, H. J. (2018). An expanded toolkit for gene tagging based on MiMIC and scarless CRISPR tagging in *Drosophila*. *eLife, e38709.* doi: 10.7554/eLife.38709.

Lindsley, D. L. & Grell, E. H. (1968). Genetic variations of *Drosophila melanogaster*. *Carnegie Institution, 627,* 472.

Lloyd, T. E., Atkinson, R., Wu, M. N., Zhou, Y., Pennetta, G., & Bellen, H. J. (2002). Hrs regulates endosome membrane invagination and tyrosine kinase receptor signaling in *Drosophila*. *Cell, 108,* 261-269.

Louvi, A., & Artavanis-Tsakonas, S. (2012). Notch and disease: a growing field. *Seminal Cell Development Biology, 23,* 473-480. doi: 10.1016/j.semcdb.2012.02.005.

Michellod, M. A., & Randsholt, N. B. (2008). Implication of the *Drosophila* beta-amyloid peptide binding-like protein AMX in Notch signaling during early neurogenesis. *Brain Research Bulletin, 75,* 305-309. doi:10.1016/j.brainresbull.2007.10.060.

Michellod, M., Forquignon, F., Santamaria, P., & Randsholt, N. B. (2003). Differential requirements for the neurogenic gene *almondex* during *Drosophila melanogaster* development. *Genesis, 37,* 113-122.

Moellering R. E., Cornejo M., Davis T. N., Del Bianco C., Aster J. C., Blacklow S. C., Kung A. L., Gilliland D. G., Verdine G. L., & Bradner J. E. (2009). Direct inhibition of the NOTCH transcription factor complex. *Nature, 462 (7270),182-188. doi:10.1038/nature08543.*

Mohler, D., & Carroll, A. (1984). Report of new mutants. *Drosophila Information Service, 60,* 236-241.

Mohler, J. D. (1977). Developmental genetics of the *Drosophila* egg. I. Identification of 59 sex-linked cistrons with maternal effects on embryonic development. *Genetics, 85,* 259-272.

Morel, V., & Schweisguth, F. (2000). Repression by Suppressor of Hairless and activation by Notch are required to define a single row of single-minded expressing cells in the *Drosophila* embryo. *Genes and Development, 14,* 377-388.

Murthy, M., Garza, D., Scheller, R. H., & Schwarz, T. L. (2003). Mutations in the exocyst component Sec5 disrupt neuronal membrane traffic, but neurotransmitter release persists. *Neuron, 37,* 433-447.

O'Neill, E. M., Rebay, I., Tjian, R., & Rubin, G. M. (1994). The activities of two Ets-related transcription factors required for *Drosophila* eye development are modulated by the Ras/MAPK pathway. *Cell, 78,* 137-147.

O'Sullivan, N. C., Jahn, T. R., Reid, E., & O'Kane, C. J. (2012). Reticulon-like-1, the *Drosophila* orthologue of the hereditary spastic paraplegia gene reticulon 2, is required for organization of endoplasmic reticulum and of distal motor axons. *Human Molecular Genetics, 21(15),* 3356-65.

Parks, A. L., Cook, K. R., & Francis-Lang, H. L. (2004). Systematic generation of high-resolution deletion coverage of the *Drosophila*

melanogaster genome. *Nature Genetics, 36,* 288-292.

Perrimon, N., & Mahowald, A. P. (1986). l(1)hopscotch, A larval-pupal zygotic lethal with a specific maternal effect on segmentation in *Drosophila*. *Developmental Biology, 118,* 28-41.

Poulson, D. (1939). Effects of Notch deficiencies. *Drosophila Information Service, 12,* 64.

Poulson, D. (1940). The effects of certain X-chromosome deficiencies on the embryonic development of *Drosophila melanogaster*. *Journal of Experimental Zoology, 83,* 271-335.

Rebay, I., Fleming, R. J., Fehon, R. G., Cherbas, L., Cherbas, P., & Artavanis-Tsakonas, S. (1991). Specific EGF repeats of Notch mediate interactions with Delta and Serrate: implications for Notch as a multifunctional receptor. *Cell, 67,* 687-699.

Rhyu, M. S., Jan, L. Y., & Jan, Y. N. (1994). Asymmetric distribution of numb protein during division of the sensory organ precursor cell confers distinct fates to daughter cells. *Cell, 76,* 477-491.

Salazar, J. L., & Yamamoto, S. (2018). Integration of *Drosophila* and human genetics to understand Notch signaling related diseases. *Advances in Experimental Medicine and Biology, 1066,* 141-185. doi: 10.1007/978-3-319-89512-3_8.

Schweisguth, F. (2004). Regulation of Notch signaling activity. *Current Biology, 14,* 129-138. doi:10.1016/j.cub.2004.01.023.

Shannon, M. P. (1973). The development of eggs produced by the female-sterile mutant *almondex* of *Drosophila melanogaster*. *Journal of Experimental Zoology, 183,* 383400.

Shannon, M. P. (1972). Characterization of the female-sterile mutant *almondex* of *Drosophila melanogaster*. *Genetica, 43,* 244-256.

Shao L., Luo Y., Moloney D. J., & Haltiwanger R (2002). O-glycosylation of EGF repeats: identification and initial characterization of a UDP-glucose: protein O-glucosyltransferase".*Glycobiology*, *12 (11),* 763–770. doi:10.1093/glycob/cwf085.

Sharma V. M., Draheim K. M., & Kelliher M. A. (2007). The Notch1/c-Myc pathway in T cell leukemia. *Cell Cycle*. *6(8),* 927–930. doi:10.4161/cc.6.8.4134.

Siebel, C., & Lendahl, U. (2017). Notch signaling in development, tissue homeostasis, and disease. *Physiological Reviews, 97(4),* 1235-1294.

Simpson P., Carteret C. (1990). Proneural clusters: equivalence groups in the epithelium of *Drosophila*. *Development 110,* 927–932.

Struhl, G., & Greenwald, I. (1999). Presenilin is required for activity and nuclear access of Notch in *Drosophila*. *Nature, 398,* 522-525. doi:10.1038/19091.

Suzuki, M., Hara, Y., Takagi, C., Yamamoto, T. S. & Ueno, N. (2010). MID1 and MID2 are required for *Xenopus* neural tube closure through the regulation of microtubule organization. *Development, 137,* 2329-39.

Takashima, S. & Murakami, R. (2001). Regulation of pattern formation in the *Drosophila* hindgut by wg, hh, dpp, and en. *Mechanical Development, 101,* 79-90.

Tamura K., Taniguchi Y., Minoguchi S., Sakai T., Tun T., Furukawa T., Honjo T. (1995). Physical interaction between a novel domain of the receptor Notch and the transcription factor RBP-J kappa/Su(H). *Current Biology, 5 (12),* 1416-1423. doi:10.1016/S0960-9822(95)00279-X.

Tanaka, T., & Nakamura, A. (2008). The endocytic pathway acts downstream of Oskar in *Drosophila* germplasm assembly. *Development, 135,* 1107-1117.

Trylinski, M., Mazouni, K., & Schweisguth, F. (2017). Intra-lineage fate decisions involve activation of Notch receptors basal to the midbody in *Drosophila* sensory organ precursor cells. *Current Biology, 27(15),* 2239-2247.e3. doi:10.1016/j.cub.2017.06.030.

Vaccari, T., Lu, H., Kanwar, R., Fortini, M. E., & Bilder, D. (2008). Endosomal entry regulates Notch receptor activation in *Drosophila melanogaster*. *Journal of Cell Biology, 180(4),* 755-62. doi: 10.1083/jcb.200708127.

Vassin, H., Bremer, K. A., Knust, E., & Campos-Ortega, J. A. (1987). The neurogenic gene *Delta* of *Drosophila melanogaster* is expressed in neurogenic territories and encodes a putative transmembrane protein with EGF-like repeats. *The EMBO Journal, 6,* 3431-3440.

Weng A. P., Ferrando A. A., Lee W., Morris J. P, Silverman L. B., Sanchez-Irizarry C., Blacklow S. C., Look A. T., & Aster J. C. (2004). Activating mutations of NOTCH1 in human T cell acute lymphoblastic leukemia. *Science, 306 (5694),* 269–271. doi:10.1126/science.1102160.

Wharton K. A., Johansen K. M., Xu T., & Artavanis-Tsakonas S. (1985). Nucleotide sequence from the neurogenic locus Notch implies a gene product that shares homology with proteins containing EGF-like repeats. *Cell, 43,* 567–581.doi:10.1016/0092-8674(85)90229-6.

Yamakawa, T., Yamada, K., Sasamura, T., Nakazawa, N., Kanai, M., Suzuki, E., Fortini, M. E., & Matsuno, K. (2012). Deficient Notch signaling associated with neurogenic *pecanex* is compensated for by the unfolded protein response in *Drosophila*. *Development, 139,* 558-567. doi:10.1242/dev.073858.

Yamamoto, S. (2019). Making sense out of missense mutations: Mechanistic

dissection of Notch receptors through structure-function studies in *Drosophila*. *Development, Growth & Differentiation.* In Press.

Yamamoto, S., Charng, W. L., & Bellen, H. J. (2010). Endocytosis and intracellular trafficking of Notch and its ligands. *Current Topics in Developmental Biology, 92*, 165-200. doi: 10.1016/S0070-2153(10)92005-X.

Yamamoto, S., Schulze, K. L., & Bellen, H. J. (2014). Introduction to Notch signaling. *Methods in Molecular Biology*, *1187*, 1-14. doi: 10.1007/978-1-4939-1139-4_1.

Yano, H., Yamamoto-Hino, M., Abe, M., Kuwahara, R., Haraguchi, S., Kusaka, I., & Goto, S. (2005). Distinct functional units of the Golgi complex in *Drosophila* cells. *Proceeding of the National Academy of Science, 102,* 38, 13467-13472. doi:10.1073pnas.0506681102.

Yuan, Z., Praxenthaler, H., Tabaja, N., Torella, R., Preiss, A., Maier, D., & Kovall, R. A. (2016). Structure and function of the Su(H)-Hairless repressor complex, the major antagonist of Notch signaling in *Drosophila melanogaster*. *PLoS Biology, 14(7),* e1002509.

6. Acknowledgements

First and foremost, I offer my sincerest gratitude to the Almighty God, for bestowing upon me to finish my Doctoral course successfully.

I would like to express my deepest gratitude to my supervisor, Prof. Kenji Matsuno (Department of Biological Sciences, Graduate School of Science, Osaka University) for giving me the precious opportunity to do PhD at Osaka University, and for all of his kind supports, crucial guidance and valuable advices during my PhD journey and during my stay in Japan.

I would like to express my heartiest thanks to my co-supervisor, Assistant Professor Dr. Tomoko Yamakawa, and other Assistant Professors Dr. Mikiko Inaki, Dr. Takeshi Sasamura (Matsuno Lab., Department of Biological Sciences, Graduate School of Science, Osaka University) for their valuable teaching, comments and suggestions on my research.

I would like to express my sincerest thanks to Professor Motoo Kitagawa (Department of Biochemistry, International University of Health and Welfare School of Medicine, Narita, Chiba, Japan) and Dr. Shinya Yamamoto (Department of Molecular and Human Genetics, Baylor College of Medicine, Houston, Texas USA) for their critics and valuable suggestion on writing my manuscript.

I would like to express my sincerest thanks to Professor Masahiro Ueda (Department of Biological Sciences, Graduate School of Science, Osaka University) and Assistant Professor Joji Mima (Institute of Protein Research, Osaka University) for their critics and valuable suggestion on my research.

I would like to express my heartiest thanks to former post-doc. fellow Satoshi Kuwana, former lab. members Kenjiroo Matsumoto, Yusuke Kamei, Tomoki Ishibashi,

Momoko Inatomi, current lab. members Yi-ting Lai, Dongsun Shin, and others for their kind help in my research.

I would like to express my sincerest gratitude for financial support to Osaka University as a research assistant (RA) and 99-Asian Scholarship Foundation that makes financially stability of my stay in Japan.

Finally, I would like to thank my family members and friends, especially my husband Dr. Suman Chandra Nath, who supported me spiritually to finish this incredible journey, “Osaka University Student Association of Bangladesh (OUSAB)” and Japanese host family for their kind support during my stay in Japan.

Puspa DAS

Laboratory of Cell Biology (Matsuno Lab)

Department of Biological Sciences

Graduate School of Science, Osaka University

1-1 Machikaneyama, Toyonaka, Osaka, 560-0043 JAPAN